13 Electromagnetic Properties of Materials

13.1 INTRODUCTION

Materials react to applied electromagnetic fields in a variety of ways including displacements of both free and bound electrons by electric fields and the orientation of atomic moments by magnetic fields. In most cases, these responses can be treated as *linear* (proportional to the applied fields) over useful ranges of field magnitudes. Often the response is independent of the direction of the applied field; the material is called *isotropic*. The responses of these linear, isotropic materials to time-varying fields may depend to a significant extent upon the frequency of the fields. The materials considered heretofore in this text have been isotropic and linear and we have been able to represent them by scalar values of ε and μ for analysis at a given frequency. Common dielectrics such as glass, fused quartz, and polystyrene and common conductors such as copper, aluminum, and brass behave this way in a vast majority of applications.

Some comment should be made here about terminology. We use the terms *dielectric, conductor*, and *magnetic material* to indicate the character of the dominant response. A study would show that in all solids and liquids the permittivity differs appreciably from that of free space as a result of the behavior of the bound electrons in the constituent atoms. In a conductor, however, the movement of the free electrons in response to the electric field produces an electromagnetic response which overwhelms that of the bound electrons. Similarly, ferromagnetic materials are mostly rather highly conductive but we refer to them as magnetic materials, as that property is the most significant in their application. All materials have some response to magnetic fields but, except for ferromagnetic and ferrimagnetic types, this is usually small, and differs from μ_0 by a negligible fraction.

The first part of the chapter deals with isotropic linear media, giving physical explanations for the electric and magnetic responses. These are necessarily qualitative or semiquantitative and in many cases incomplete, since detailed analysis requires quantum mechanics. Conductive materials are reasonably well represented by a free-electron model; we introduce it as a simple vehicle to show how the complex permittivity comes

out of first principles. A section is devoted to clarifying the meaning we have given to a *perfect conductor* and to distinguishing it from a *superconductor*.

Important device applications depend upon the nonlinear behavior of certain materials. These include conversion of energy from one frequency to another, for example, frequency multipliers for the mixing of two signals of different frequencies to give a third. The nonlinear, hysteretic behavior and extremely high permeability of ferromagnetic materials significantly determine their use.

The final portion of the chapter treats anisotropic materials, both from the view of the physical sources of the anisotropy and with regard to calculating wave propagation in such media. Dielectric crystals with permittivity that depends upon the orientation of the electric field can be described succinctly by a so-called *dielectric ellipsoid.* This is introduced, and wave propagation in such crystals is discussed. Ferrites (ferrimagnetic solids) and plasmas (ionized gases with equal positive and negative charge densities) situated in a steady magnetic field exhibit a type of anisotropy in which characteristic propagating waves are circularly polarized. That the behavior depends on the propagation direction relative to the magnetic field leads to the possibility of nonreciprocal microwave and optical devices.

Linear Isotropic Media

13.2 Characteristics of Dielectrics

In this section we consider linear, isotropic dielectrics to explain the connection between microscopic effects and their representation by a permittivity. It is of special importance to discuss the frequency dependence of permittivity. We consider here usual dielectrics with $\mu = \mu_0$.

We saw in connection with the Poynting theorem in Sec. 3.12 that currents in phase with the electric field (there considered to be conduction currents) lead to an energy-loss term. In the general characterization of lossy dielectrics we introduce a complex permittivity

$$\varepsilon = \varepsilon' - j\varepsilon'' \tag{1}$$

which enters Maxwell's equations as the current $j\omega(\varepsilon' - j\varepsilon'')\mathbf{E}$, the second term of which is in phase with electric field. Both ε' and ε'' are, in general, functions of frequency. The various physical phenomena contributing to ε' and ε'' differ for solids, liquids, and gases and are too complicated to summarize here in any detail. Several

excellent books and survey articles give thorough treatments.[1–6] Nevertheless, discussion of some of the properties and the simple models for these help to give insight into the most important characteristics.

It can be shown that, if the atoms or molecules are polarized (or their natural dipole moments have a nonzero average alignment), a dipole moment density can be defined by

$$\mathbf{P}_d = \lim_{\Delta V \to 0} \frac{\Sigma_i \mathbf{p}_i}{\Delta V}$$

and that this, neglecting higher-order multipoles, is identical to the so-called *polarization*[7] that enters the relation between $\mathbf{D}$ and $\mathbf{E}$:

$$\mathbf{D} = \varepsilon_0 \mathbf{E} + \mathbf{P} = \varepsilon_0(1 + \chi_e)\mathbf{E} \tag{2}$$

The term χ_e is the dielectric susceptibility and we have assumed that the polarization is linearly dependent on the field $\mathbf{E}$. A few dielectrics, such as electrets,[8] have a permanent polarization, but we are chiefly concerned with dielectrics in which $\mathbf{P}$ is induced by the applied electric field $\mathbf{E}$ and shall consider only these in the following. If there are N like molecules per unit volume, the induced polarization may be written

$$\mathbf{P} = \varepsilon_0 \chi_e \mathbf{E} = N\alpha_T \mathbf{E}_{loc} = N\alpha_T g \mathbf{E} \tag{3}$$

where α_T is the *molecular polarizability*, and g, the ratio between local field $\mathbf{E}_{loc}$ acting on the molecule and the applied field $\mathbf{E}$. The local field differs from applied field because of the effect of surrounding molecules. We also write electric flux density as

$$\mathbf{D} = \varepsilon \mathbf{E} = \varepsilon_0 \varepsilon_r \mathbf{E} \tag{4}$$

so by comparing with (2) and (3) we may write relative permittivity

$$\varepsilon_r = 1 + \frac{N\alpha_T g}{\varepsilon_0} = 1 + \chi_e \tag{5}$$

1 *C. Kittel,* Introduction to Solid State Physics, *6th ed., Wiley, New York, 1986.*

2 *N. W. Ashcroft and N. D. Mermin,* Solid State Physics, *Holt, Rinehart and Winston, New York, 1976.*

3 *B. K. P. Scaife,* Principles of Dielectrics, *Oxford University Press, Oxford, UK, 1989.*

4 *E. D. Palik (Ed.),* Handbook of Optical Constants of Solids, *Academic Press, Orlando, FL, 1985.*

5 *E. D. Palik (Ed.),* Handbook of Optical Constants of Solids II, *Academic Press, Boston, MA, 1991.*

6 *D. E. Gray (Ed.),* American Institute of Physics Handbook, *3rd ed., McGraw-Hill, New York, 1972.*

7 *Not to be confused with polarization of a wave in the sense of Sec. 6.3. See footnote to Sec. 6.3.*

8 *Electrets are readily formed in the laboratory by applying a dc electric field across certain types of molten wax and allowing the resulting dipoles to "freeze in" as the wax solidifies. For a bibliography on electrets see B. Gross,* Charge Storage in Solid Dielectrics, *Elsevier, Amsterdam, 1964.*

If the surrounding molecules act in a spherically symmetric fashion on the molecule for which $\mathbf{E}_{loc}$ is being calculated, g can be shown to be $(2 + \varepsilon_r)/3$ and (5) may then be written as

$$\frac{\varepsilon_r - 1}{\varepsilon_r + 2} = \frac{N\alpha_T}{3\varepsilon_0} \tag{6}$$

This expression is known as the Clausius–Mossotti relation or, when frequency effects in α_T are included, the Debye equation. It is most accurate for gases but does give qualitative behavior for liquids and solids.

The molecular polarizability α_T, defined above, has contributions from several different atomic or molecular effects. One part, called electronic, arises from the shift of the electron cloud in each atom relative to its positive nucleus, much as was pictured in Sec. 1.3. Another part, called ionic, comes from the displacement of positive and negative ions from their neutral positions. Still another part may arise if the individual molecules have permanent dipole moments. Application of the electric field tends to align these permanent dipoles against the randomizing forces of molecular collision, and since random motion is a function of temperature, this last effect is clearly temperature dependent. The three effects together constitute the total molecular polarizability,

$$\alpha_T = \alpha_e + \alpha_i + \alpha_d \tag{7}$$

where α_e, α_i, and α_d are electronic, ionic, and permanent dipole contributions, respectively.

Frequency Effects In the classical model of the electronic polarization, any displacement of the charge cloud from its central ion produces a restoring force and its interaction with the inertia of the moving charge cloud produces a resonance as in a mechanical spring-mass system. Similarly, the displacement of one ion from another produces resonances in the ionic polarizability but at lower frequencies than for the electronic contribution because of the larger masses in motion. There are also losses or damping in each of the resonances, pictured as arising from radiation or interaction with other charges. The Lorentz model of an atom in which damping is proportional to the velocity of the oscillating charge cloud is expressed by the equation of motion for displacement:

$$\frac{d^2r}{dt^2} + \Gamma\frac{dr}{dt} + \omega_0^2 r = -\frac{e}{m}E_{loc} \tag{8}$$

where Γ is a damping constant and ω_0 is related to the restoring force. Assuming the field and displacement in phasor form, one finds

$$r = \frac{-(e/m)E_{loc}}{(\omega_0^2 - \omega^2) + j\omega\Gamma} \tag{9}$$

The electronic polarizability is the ratio of the dipole moment $p = -er$ to the local field:

$$\alpha_e = \frac{(e^2/m)}{(\omega_0^2 - \omega^2) + j\omega\Gamma} \tag{10}$$

We can generalize this to represent all electronic and ionic resonant responses:

$$\alpha_j = \frac{F_j}{(\omega_j^2 - \omega^2) + j\omega\Gamma_j} \tag{11}$$

where F_j measures the strength of the jth resonance. This has the form of the impedance of a parallel resonant circuit. Real and imaginary parts of the expression contribute to ε' and ε'', respectively, in a manner shown by the electronic and ionic resonances pictured for a hypothetical dielectric in Fig. 13.2*a*. Near a resonance the lossy part goes through a peak. The contribution to ε' from a given resonance, like the reactance of the tuned circuit, has peaks of opposite sign on either side of the resonance.

The dynamic response of the permanent dipole contribution to permittivity is different in that the force opposing complete alignment of the dipoles in the direction of the applied field is that from thermal effects. It acts as a viscous force and the dynamic response is "overdamped." The frequency response of such an overdamped system is of the form

$$\alpha_d = \frac{p^2}{3k_B T(1 + j\omega\tau)} \tag{12}$$

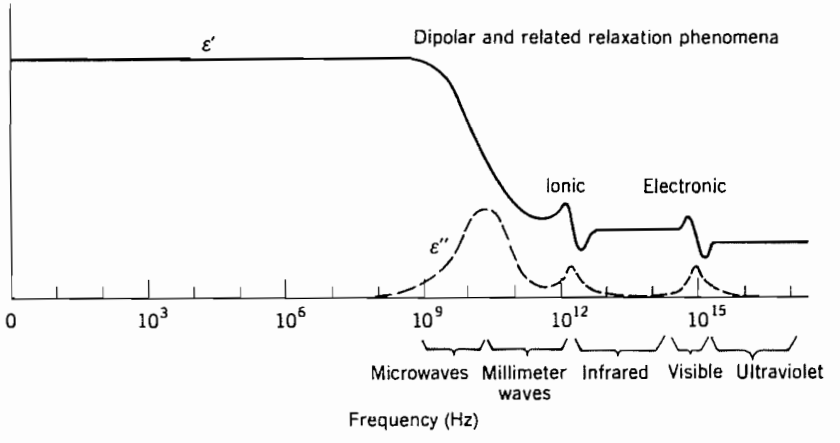

FIG. 13.2*a* Frequency response of permittivity and loss factor for a hypothetical dielectric showing various contributing phenomena.

where T is temperature, k_B is Boltzmann's constant, p is the permanent dipole moment, and τ is a relaxation time for the effect (i.e., the time for polarization to fall to $1/e$ of the original value if orienting fields are removed). Dipole contributions are also illustrated for the hypothetical dielectric of Fig. 13.2*a* and produce smoother decreases in ε as one goes through the range $\omega\tau \sim 1$, along with a peak of absorption. The picture of dipole orientation and relaxation as given applies best to gases and liquids possessing such dipoles, but there are a variety of similar relaxation effects in solids.

Relation Between Real and Imaginary Parts of Permittivity The analytic properties of the complex permittivity defined by (1) provide certain relationships between $\varepsilon'(\omega)$ and $\varepsilon''(\omega)$ so that the frequency behavior of one part is not independent of the frequency behavior of the other. These interesting and important relationships, known as the Kramers–Kronig relations,[9] may be written

$$\varepsilon'(\omega) = \varepsilon_0 + \frac{2}{\pi} P \int_0^\infty \frac{\omega' \varepsilon''(\omega') d\omega'}{(\omega'^2 - \omega^2)} \tag{13}$$

$$\varepsilon''(\omega) = -\frac{2\omega}{\pi} P \int_0^\infty \frac{[\varepsilon'(\omega') - \varepsilon_0]\, d\omega'}{\omega'^2 - \omega^2} \tag{14}$$

where P denotes that the principal value of the integral should be taken. They are similar to relations between resistance and reactance functions of frequency in circuit theory (see Sec. 11.11).

At optical frequencies it is common to use the index of refraction defined by Eq. 6.2(28) rather than permittivity. This also is complex for a material with losses (absorption). With $\mu = \mu_0$,

$$n_c(\omega) = n_r(\omega) - jn_i(\omega) = \{[\varepsilon'(\omega) - j\varepsilon''(\omega)]/\varepsilon_0\}^{1/2} \tag{15}$$

(n_r and n_i are often listed as n and k, respectively in optical tables but, to avoid confusion with wavenumber, we use the self-defining n_i for the *extinction coefficient* k.)

Values of $\varepsilon'/\varepsilon_0$ and $\varepsilon''/\varepsilon'$ for some representative materials at radio and microwave frequencies were given in Table 6.4a. Values of refractive index n_r are plotted versus wavelength for several optical materials in Fig. 13.2*b*. The imaginary part n_i is generally small except in or near absorption bands, where it is a strong function of wavelength. The references[4–6] give curves for numerous materials in their absorption regimes.

13.3 Imperfect Conductors and Semiconductors

A *good conductor* was defined in Chapter 3 as one that follows Ohm's law and for which displacement current is negligible compared with conduction current. In that case the current and electric field are in phase. There are a number of important materials and situations in which the currents can have significant components at phase quadrature

[9] *J. D. Jackson, Classical Electrodynamics, 2nd ed., p. 311, Wiley, New York, 1975.*

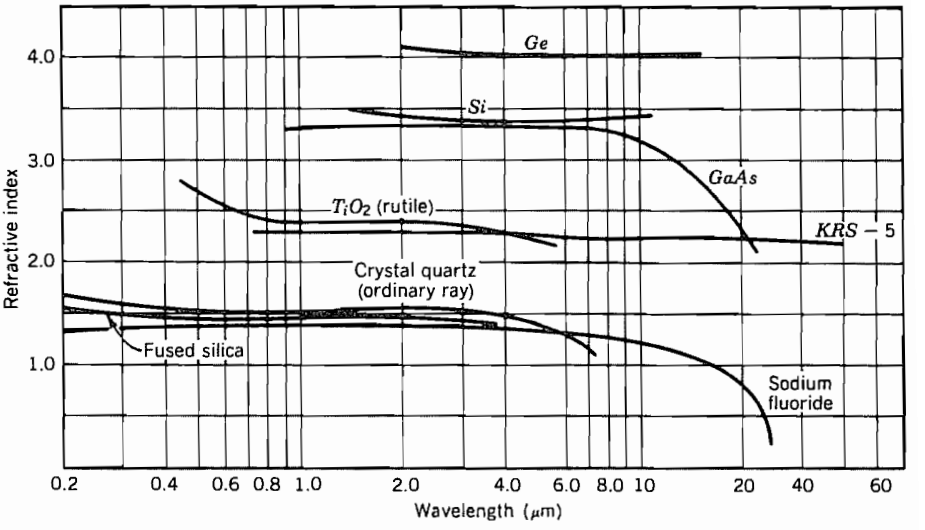

FIG. 13.2*b* Refractive index versus wavelength for several materials with useful values of optical and infrared transparency. Data from *American Institute of Physics Handbook*.[6]

to the electric field. At higher frequencies the displacement current becomes increasingly important; for example, at microwave frequencies semiconductors can have comparable conduction and displacement currents. Also, at optical frequencies the charge motion in metals can give current components both in phase with the electric field and at phase quadrature. The latter has the same effect as a displacement current and is included in the real part of the permittivity.

Let us consider a medium consisting of a density n_e of free electrons with a background of fixed positive ions of the same density. This can be considered to be a model of a conductor, semiconductor, or an ionized gas (plasma); only the values of the parameters are different. For most cases of interest, the derived complex permittivity will be used to study the behavior of TEM or quasi-TEM waves; we will use that fact to justify certain simplifications of the analysis.

The force on charges arising from interactions with the magnetic field in a wave is typically several orders of magnitude smaller than the electric forces (Prob. 13.3a), so we will neglect the former. In this analysis we bring in the effect of collisions by introducing a term representing the resulting average rate of loss of momentum. The equation of motion for an average electron is then

$$m\frac{d\mathbf{v}}{dt} = -e\mathbf{E} - m\nu\mathbf{v} \tag{1}$$

If it is assumed that each collision causes a total loss of momentum of the electron, then ν is the collision frequency.

The total time derivative is taken as we move with the particle and must in general be written as

$$\frac{d\mathbf{v}}{dt} = \frac{\partial \mathbf{v}}{dt} + \frac{\partial \mathbf{v}}{\partial x}\frac{dx}{dt} + \frac{\partial \mathbf{v}}{\partial y}\frac{dy}{dt} + \frac{\partial \mathbf{v}}{\partial z}\frac{dz}{dt} \tag{2}$$

To simplify, consider a uniform plane wave propagating in the z direction so that the field is transverse and all velocity components are also in transverse directions. Thus the last term of (2), which contains the z-directed velocity dz/dt, vanishes. By virtue of the assumed uniformity of the fields in the transverse plane, the variations of velocity with respect to x and y are zero. Hence the total and partial derivatives with respect to time are equal here. Since we are considering the steady-state behavior of the system we may let $\mathbf{E} = \mathbf{E}e^{j\omega t}$ and $\mathbf{v} = \mathbf{v}e^{j\omega t}$. Equation (1) may then be arranged to give the velocity in terms of the electric field as

$$\mathbf{v} = \frac{-e\mathbf{E}}{m(\nu + j\omega)} \tag{3}$$

The electron density n_e is undisturbed by the motions of the electrons since all paths lie in the transverse planes and are parallel with each other. Then the convection current density is

$$\mathbf{J} = -n_e e\mathbf{v} = \frac{n_e e^2 \mathbf{E}}{m(\nu + j\omega)} \tag{4}$$

This can be inserted in Maxwell's curl equation, $\nabla \times \mathbf{H} = j\omega\varepsilon_1\mathbf{E} + \mathbf{J}$:

$$\begin{aligned} \nabla \times \mathbf{H} &= j\omega\varepsilon_1\mathbf{E} + \frac{n_e e^2 \mathbf{E}}{m(\nu + j\omega)} \\ &= j\omega\left[\left(\varepsilon_1 - \frac{n_e e^2}{m(\nu^2 + \omega^2)}\right) - j\frac{n_e e^2 \nu}{\omega m(\nu^2 + \omega^2)}\right]\mathbf{E} \end{aligned} \tag{5}$$

where ε_1 is used in the displacement current term to represent the effect of the bound electrons of the positive ion background. It is assumed for conductive materials to have an insignificant imaginary part of ε_1 compared with the effect of $\mathbf{J}$. Separating the real and imaginary parts of the right-hand side, we can identify the components of the complex permittivity $\varepsilon = \varepsilon' - j\varepsilon''$. Thus,

$$\varepsilon' = \varepsilon_1 - \frac{n_e e^2}{m(\nu^2 + \omega^2)} \tag{6}$$

and

$$\varepsilon'' = \frac{n_e e^2 \nu}{\omega m(\nu^2 + \omega^2)} \tag{7}$$

Note that $n_e e^2/m\nu$ is the low-frequency conductivity σ.

One important application of the above results is to materials with moderate to low conductivity (say, $\sigma \lesssim 1$ S/m) such as semiconductors with moderate doping. Then

for microwave and millimeter-wave frequencies where $\omega^2 \ll \nu^2$, the second term in (6) is negligible and ε becomes

$$\varepsilon = \varepsilon_1 - j\frac{\sigma}{\omega} \tag{8}$$

which is the form used in Eq. 6.4(11).

At the other extreme is the ionized gas with very low density and negligible collision frequency. In that case we can take $\varepsilon_1 = \varepsilon_0$ and $\varepsilon'' = 0$ so that

$$\varepsilon = \varepsilon_0\left(1 - \frac{\omega_p^2}{\omega^2}\right) \tag{9}$$

where ω_p is the so-called *plasma frequency*:

$$\omega_p = \sqrt{\frac{n_e e^2}{\varepsilon_0 m}} \tag{10}$$

The physical meaning of the plasma frequency is as follows: if alternate plane layers of compression and rarefaction of the electrons in a uniform positive ion background were set as initial conditions, the charge would subsequently oscillate at the plasma frequency because of the interaction of forces between charges and the inertial effects.

An immediate observation about the form (9) for permittivity is that it is negative for all frequencies below the plasma frequency. Therefore, the intrinsic wave impedance $\eta = \sqrt{\mu/\varepsilon}$ is imaginary, so that a wave with $\omega < \omega_p$ incident from free space on a region of ionized gas is reflected. This is also seen from the propagation constant, Eq. 6.2(25), which becomes, for the plasma described by (9),

$$k^2 = \omega^2\mu\varepsilon_0\left(1 - \frac{\omega_p^2}{\omega^2}\right) \tag{11}$$

If $\omega < \omega_p$, k^2 is negative so $jk = \alpha$ and $\beta = 0$. Then

$$E_x = E_+ e^{-\alpha z} + E_- e^{\alpha z} \tag{12}$$

That is, purely attenuated waves exist for $\omega < \omega_p$. For frequencies higher than ω_p, k^2 is positive and unattenuated waves propagate in the gas. The ω–β diagram for TEM waves in an ionized gas is shown in Fig. 13.3*a*.

The effect described above for a plasma can also be observed in some metals (e.g., aluminum and the alkali metals) at optical frequencies. Very high fractional reflection is observed for frequencies below the plasma frequency, which is typically between the visible and ultraviolet ranges. The effects in metals are actually more complex than the simple model above would suggest and a complete treatment requires quantum mechanics. As noted in Eq. 13.2(15), the properties at optical frequencies are usually expressed by a complex index of refraction n_c. Both parts of n_c may vary appreciably with frequency, the variation being a characteristic of the particular metal. Curves for silver and nickel for a part of the visible and infrared ranges are shown in Fig. 13.3*b*.

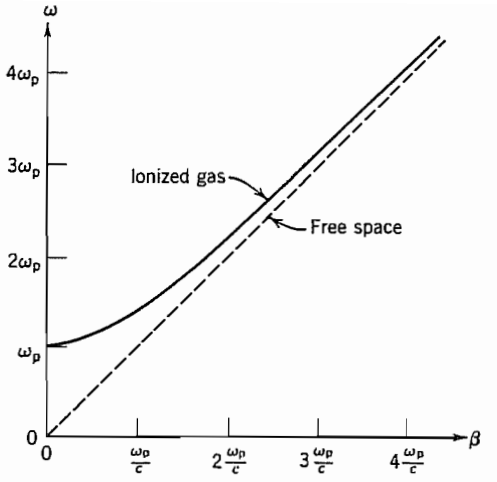

FIG. 13.3*a* The ω–β diagram for a plane wave propagating through an ionized gas.

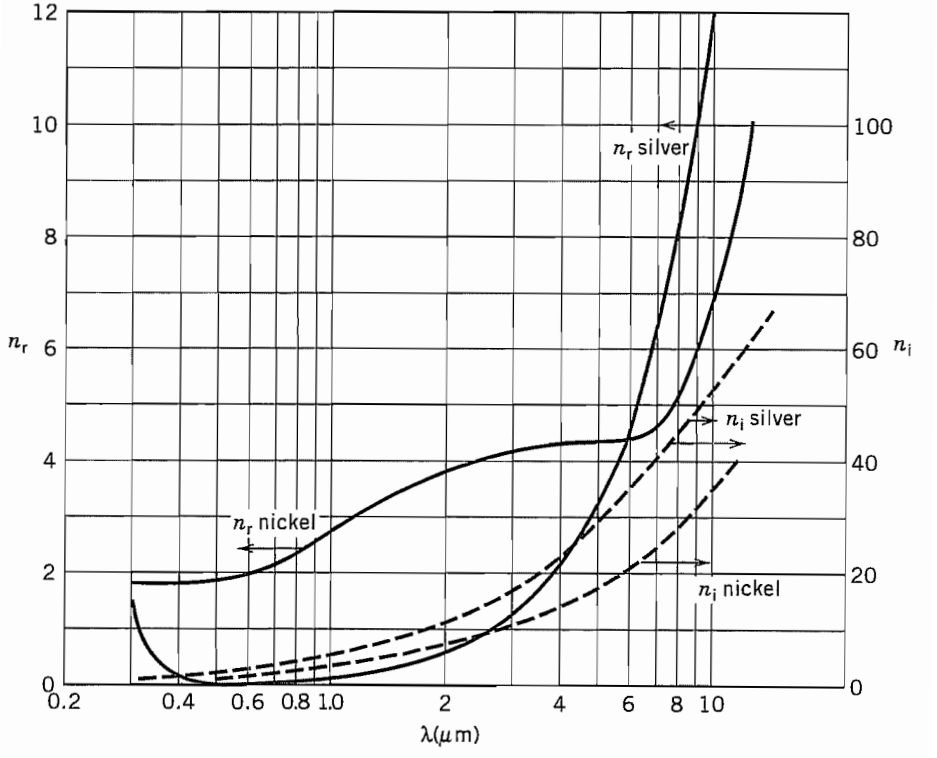

FIG. 13.3*b* Real and imaginary parts of refractive index for silver and nickel over a part of the optical range. (Data from *Handbook of Optical Constants of Solids*.[4])(Measured values depend strongly on surface conditions.)

13.4 Perfect Conductors and Superconductors

At numerous points in this text—and very commonly in electromagnetic theory—we refer to *perfect conductors*. Here we wish to comment on what is and what is not meant by that term and to see how it relates to *superconductors*.

A perfect conductor is usually understood to be a material in which there is no electric field at any frequency. Maxwell's equations ensure that there is then also no time-varying magnetic field in the perfect conductor. On the other hand, a truly static magnetic field should be unaffected by conductivity of any value, including infinity. In all time-invariant electric problems, the use of the perfect conductor approximation for an electrode ensures uniform potential over its surface. This is often an excellent approximation to a metal electrode even in problems with direct current flowing (e.g., a metal electrode on a semiconductor). In rf problems the fields are essentially zero a few skin depths inside the surface of a metal electrode. If the spacing between electrodes in the system being analyzed is much greater than the skin depth, the perfect conductor assumption that $\mathbf{E} = 0$ at the surface is a good one for finding field distributions, though the penetration of the fields cannot be neglected if losses are to be found.

The real approximation to the perfect conductor would be a conductor in which the collision frequency approaches zero. This was believed to be the correct model for a superconductor in the period between its discovery in 1911 by H. Kamerlingh Onnes and the experiment by W. Meissner and R. Ochsenfeld in 1933.[10] A collisionless conductor can be modeled as a dense plasma and the results of the preceding section may be applied with $\nu = 0$. For frequencies below the plasma frequency, Eq. 13.3(12) indicates that the fields inside the conductor (Fig. 13.4) can exist only near the surface where they are excited. This phenomenon is like the skin effect (Sec. 3.16) except that here the behavior of the shielding currents is determined by inertia of the electrons rather than collisions. For frequencies a factor of about 10 or more below the plasma frequency, the attenuation factor $\alpha = (\mu n_e e^2/m)$ is independent of frequency and has values typically on the order of $(0.1\ \mu\text{m})^{-1}$ so the interior of bulk samples can be considered essentially free of time-varying fields. The results of the plasma wave analysis appear to be valid to zero frequency; however, in static fields in the absence of collisions, the electrons would be accelerated to infinite velocities and the analysis is not applicable.

Extremely pure crystals of metal can have very low collision frequencies at temperatures near the absolute zero, but such materials are not of much interest in practice since it is difficult to construct useful systems of single metal crystals. On the other hand, the superconductor is a realizable candidate. The ideal collisionless conductor excludes time-varying fields but the experiment of Meissner and Ochsenfeld on a superconductor showed that constant magnetic fields are also excluded from the interior. The London theory (1935) showed that this result would be obtained if

$$\nabla \times \mathbf{J} = -\Lambda \mathbf{B} \tag{1}$$

[10] *T. Van Duzer and C. W. Turner,* Principles of Superconductive Devices and Circuits, *Elsevier, New York, 1981. (To be reissued by Prentice Hall.)*

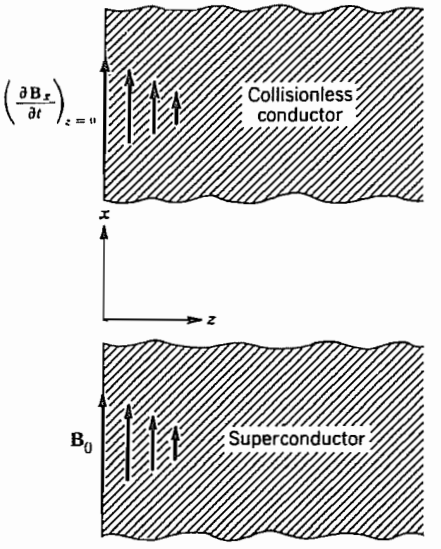

FIG. 13.4 Coordinates for analysis of fields at surface of a half-space of collisionless conductor or superconductor.

where $\Lambda = n_e e^2/m$ at $T = 0$. Substituting (1) in Maxwell's curl **H** equation and neglecting displacement current, one finds

$$\nabla \times \nabla \times \mathbf{B} = -\mu\Lambda\mathbf{B} \tag{2}$$

Using a vector identity and $\nabla \cdot \mathbf{B} = 0$ in (2) yields

$$\nabla^2\mathbf{B} - \mu\Lambda\mathbf{B} = 0 \tag{3}$$

This can be applied to the fields inside the surface of a superconductor by considering a half-space of superconductor filling $z \geq 0$ as in Fig. 13.4. We assume that only an x component of **B** exists and it varies only in the z direction. Then (3) becomes

$$\frac{d^2B_x}{dz^2} - \frac{B_x}{\lambda_L^2} = 0 \tag{4}$$

where $\lambda_L = (m/\mu n_e e^2)^{1/2}$ at $T = 0$ and is called the *London penetration depth.*[11] The solution that remains bounded is

$$B_x = B_{x0}e^{-z/\lambda_L} \tag{5}$$

which is the same as the form in Eq. 13.3(12). Typical experimentally determined penetration depths lie in the range 50–200 nm. An important difference between the superconductor and the ideal collisionless conductor is that (5) applies even for static magnetic field.

[11] *Since $\mu \approx \mu_0$ for almost all superconductive materials the definition of λ_L is usually given in terms of μ_0.*

The phenomena of superconductivity require the materials to be held at temperatures approaching the absolute zero.[10] Most superconductors are metallic elements, compounds, or alloys and make transitions into the superconducting state at critical temperatures below about 23 K. Niobium has the highest critical temperature (9.2 K) of any element, and alloys and compounds of niobium with higher critical temperatures are used widely in applications. In 1986, a new family of superconductors based on oxides was discovered to have much higher transition temperatures.[12] A series of discoveries in the following 2 years revealed other oxide materials with critical temperatures as high as 125 K. In contrast to metallic superconductors, the higher-temperature oxide superconductors are very anisotropic, with the strongest superconductive behavior in planes. When these materials are used in microwave structures, for example, thin-film transmission lines (Sec 8.6) or resonators (Sec. 10.6), the planes are formed parallel to the surface to facilitate current flow in the required direction.

The penetration depth in (5) applies for dc magnetic fields, but is also the skin depth for electromagnetic waves for frequencies well into the millimeter-wave range. This invariance of penetration is responsible for superconductive transmission lines being nearly nondispersive. Unlike the ideal collisionless conductor, losses occur in superconductors at nonzero frequencies and nonzero temperatures. These losses occur because some of the conduction electrons are not in the superconducting state and the penetrating fields can cause them to have dissipative collisions. The losses, however, are far smaller than in normal metals such as copper or gold for frequencies throughout the microwave range.

In summary, the commonly used concept of a perfect conductor ($\mathbf{E} = 0$ inside) is a convenient artifice for calculation of the field distributions outside when the actual conductor has a field penetration that is small compared with the space between conductors. This is true for either a highly conductive electrode with a small skin depth or a superconductor; however, neither a conductor nor a superconductor has exactly zero $\mathbf{E}$ inside, near the surface. To find field distributions where the spacing between electrodes is comparable with or smaller than the depth of field penetration, the latter must be taken into account. For example, some parallel-film structures in superconductive integrated circuits have insulating spacings that are much smaller than the skin depth, so wave propagation is dominated by the properties of the superconductors.

13.5 Diamagnetic and Paramagnetic Responses

As noted in Sec. 13.1, all materials have some response to magnetic fields. Except for certain categories which we will consider separately (ferromagnetic and ferrimagnetic), the magnetic response is very weak. Magnetic response can either decrease or increase the flux density for a given $\mathbf{H}$. If $\mathbf{B}$ is decreased, the material is said to be *diamagnetic*; if increased, it is called *paramagnetic*.

Atoms have a diamagnetic response that arises from changes of the electron orbits

[12] *V. Z. Kresin and S. A. Wolf,* Fundamentals of Superconductivity, *Plenum, New York, 1990.*

when the magnetic field is applied. As we saw in our study of Faraday's law, an electric field is produced by a changing magnetic field. That field induces currents which, in turn, produce a magnetic field that opposes the change. The response of the electron orbits in an atom is of this kind. The effect produces fractional changes of μ from μ_0 by only 10^{-8} to 10^{-5}.

The diamagnetic response is usually obscured in materials having natural net magnetic dipole moment. Such materials give a paramagnetic response which can arise from dipole moments in atoms, molecules, crystal defects, and conduction electrons. The dipole moments tend to align with the magnetic field but are deflected from complete alignment by their thermal activity. The fields resulting from the partially aligned dipoles add to the applied field.

If there are induced magnetic dipoles in the atoms or there is a nonzero average alignment of natural dipoles, a *dipole density* can be defined by

$$\mathbf{M} \triangleq \lim_{\Delta V \to 0} \frac{\Sigma_i \mathbf{m}_{0i}}{\Delta V} \tag{1}$$

and this is identical to the so-called *magnetization* that enters the relation between $\mathbf{B}$ and $\mathbf{H}$:

$$\mathbf{B} = \mu_0(\mathbf{H} + \mathbf{M}) \tag{2}$$

It can be shown[13] that the magnitude of the magnetization can be expressed in terms of the magnetic field $\mathbf{H}_i$ acting on the atomic dipoles and the absolute temperature T by

$$M = Nm_0\left(\coth \frac{m_0\mu_0 H_i}{k_B T} - \frac{k_B T}{m_0\mu_0 H_i}\right) \tag{3}$$

where N is the number of dipoles per unit volume, m_0 is the natural dipole moment, and k_B is Boltzmann's constant. Equation (3) is derived from considerations of the statistical distribution of the dipole orientations. The direction of $\mathbf{M}$ is parallel with $\mathbf{H}_i$ in materials of this type, and the molecular field $\mathbf{H}_i$ is negligibly different from the macroscopic field. For magnetic fields that are not too strong and temperatures not too low, the parentheses in (3) may be approximated by the first term in its series expansion. In this case the magnetization is linearly dependent on the applied field:

$$\mathbf{M} = \chi_m \mathbf{H} \tag{4}$$

and

$$\chi_m \cong \frac{N\mu_0 m_0^2}{3k_B T} \tag{5}$$

In a variety of materials at room temperature χ_m has values on the order of 10^{-5}.

Some of the most important of magnetic properties are those that involve coupling effects between atomic magnetic moments; these are discussed in the following section.

[13] *J. R. Reitz and F. J. Milford,* Foundations of Electromagnetic Theory, *Chap. 11, Addison-Wesley, Reading, MA, 1960.*

Nonlinear Isotropic Media

13.6 Materials with Residual Magnetization

If the temperature of a paramagnetic substance is reduced below a certain value, which depends on the material, the magnetization $\mathbf{M}$ may be sufficient to produce the field necessary to hold the dipoles aligned even when the external field is not present. The molecular field produced by the magnetization is[13]

$$\mathbf{H}_i = \kappa \mathbf{M} \tag{1}$$

But from Eq. 13.5(3) it is seen that a second relation between $\mathbf{H}_i$ and $\mathbf{M}$ exists. Equating M of the two expressions, the conditions for spontaneous magnetization are obtained. The temperature below which a material exhibits spontaneous magnetization is called its *Curie temperature*. From experimental knowledge of the Curie temperatures for various materials, it has been found that κ, the factor measuring the interaction of neighboring dipoles, must be on the order of 1000. On the basis of purely magnetic interactions, it would be expected to be about one-third, as in the corresponding factor for electric dipoles. The values are explained using quantum-mechanical considerations on the basis of electric interaction between molecules resulting from distortions of the charge distributions in the molecules. In some materials it is energetically favorable for dipoles to align parallel to their neighbors; these are called *ferromagnetic* substances. In some other materials it is energetically favorable for neighboring dipoles to assume an antiparallel orientation, as indicated in Fig. 13.6*a*; these are called *antiferromagnetic* substances. In *ferrimagnetic* materials, also called *ferrites*, the neighboring dipoles are aligned in an antiparallel arrangement but different types of atoms are present and the dipoles do not cancel. This is illustrated schematically in Fig. 13.6*b*.

From the foregoing discussion, one would expect that a single crystal of ferromagnetic or ferrite material would act as a permanent magnet with a common alignment of molecular dipoles. However, except in the case of very small crystals, it is energetically favorable to subdivide into regions, called *domains*, within which the dipoles are all parallel.[14] The subdivision is the one that minimizes the total energy of the crystal, which includes energy in the walls between domains and stored magnetic energy both within and outside the crystal. Figure 13.6*c* shows a photograph made by a special technique that reveals the domains in a single crystal of nickel. Note that the arrows indicating the magnetization vectors of the domains tend to cancel each other when averaged over the crystal. There are factors such as crystal shape, energetically preferred crystal directions, and the magnetic history of the sample that lead to nonzero net magnetization. (The existence of domains in thin films in the presence of an applied field is exploited for the so-called *bubble memory* devices for computer memories.[15]

[14] *C. Kittel,* Introduction to Solid State Physics, *6th ed., pp. 448–456, Wiley, New York, 1986.*
[15] *H. Jouve,* Magnetic Bubbles, *Academic Press, San Diego, CA, 1987.*

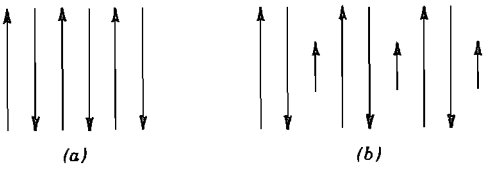

FIG. 13.6 (*a*) Arrangement of dipoles in antiferromagnetic material. (*b*) Unbalanced antiparallel dipoles in ferrites.

Practical materials ordinarily contain large numbers of crystallites with random orientations so that the macroscopic effects are isotropic. Within each crystallite is a domain structure of the type shown in Fig. 13.6*c*. When a magnetic field is applied, the walls of the domains move in such a way as to enlarge those having components of their dipole vectors in the direction of the magnetic field. If the magnetic field intensity is further increased, the dipole direction for each domain as a whole rotates toward the direction of the applied magnetic field. This process is nonlinear in that the magnetization and hence the flux density **B** are not simply proportional to the applied field. The magnetization tends to lag the field intensity, with the result that the relation between **B** and **H** has the pattern shown in Fig. 13.6*d*, which is called a *hysteresis loop*. The linear parts of the loop at high values of magnetic field correspond to the condition in which essentially all of the dipole moments are aligned, and ΔB and ΔH are therefore related by μ_0 (neglecting diamagnetic effects).

The processes of wall movement and rotation of the domains require the expenditure of energy. The energy required for the traversal of the loop by varying **H** from a large negative value to a large positive value and back again can be found from the expression

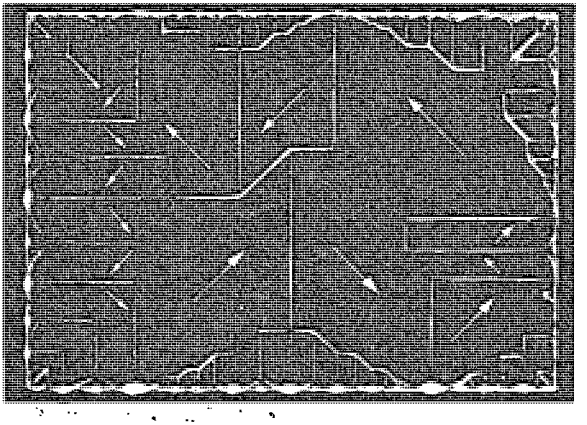

FIG. 13.6*c* Ferromagnetic domains in a single-crystal platelet of nickel. [From C. Kittel.[1] © John Wiley and Sons, 1986, New York. Original photograph from R. W. de Blois, *J. Appl. Phys.* **36**, 1647 (1965).]

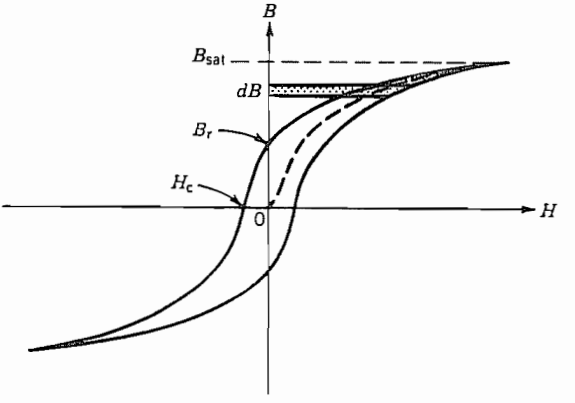

FIG. 13.6*d* Typical hysteretic B–H curve for a ferromagnetic material.

for the stored magnetic energy, Eq. 2.16(1), repeated here for convenience. The change of energy for a differential change **dB** is

$$dU_H = \int_V \mathbf{H} \cdot \mathbf{dB}\, dV \tag{2}$$

where the integration is over the volume of the material. This differential energy is shown as a shaded bar on the hysteresis loop in Fig. 13.6*d*. When the field is decreased, a portion of the energy indicated by the part of the bar outside the loop is returned to the field. The result of integrating around the loop is that the total expended energy per unit volume is equal to the area of the loop.

Some important applications of ferromagnetic materials include permanent magnets, signal recording tapes and disks, magnetic shielding, and cores for electromagnets, transformers, electric motors, and generators. These materials can be roughly divided into categories called *hard* and *soft*. The designations refer to permanence of magnetization when the applied field is removed, with hard materials retaining a strong magnetization.

Hard materials generally have a wide, rectangular hysteresis loop. Two important points on the hysteresis loop for hard materials are the *remanence* B_r and the *coercive force* H_c (see Fig. 13.6*d*). The remanence is the flux density that remains in the material when H is reduced to zero and is the value existing in a permanent magnet. The coercive force is the magnetic field that must be applied in the opposite direction to reduce the flux density to zero. Its importance lies in the fact that the retention of magnetization in the presence of disturbances (thermal, mechanical, etc.) improves with increasing coercive force. The properties of some technically important materials for permanent magnets are listed in Table 13.6a.[16]

[16] *A. H. Morrish,* The Physical Principles of Magnetism, *Robert E. Krieger, Malabar, FL, 1982.*

Table 13.6a
Hard Magnetic Materials

Material	Comment or Percent Composition	Remanence B_r (T)	Coercive Force H_c (A m^{-1})
Iron	Bonded powder	0.6	0.0765
Iron–cobalt	Bonded powder	1.08	0.0980
Alnico V	14 Ni, 8 Al, 24 Co, 3 Cu, 51 Fe	1.27	0.0650
Ticonol II	15 Ni, 7 Al, 34 Co, 4 Cu, 5 Ti, 35 Fe	1.18	0.1315

Soft materials should usually have large *saturation induction* (B_{sat} in Fig. 13.6*d*), small coercive force, large *initial permeability* (dB/dH at $B = H = 0$), large *maximum permeability* (maximum B/H), and small hysteresis losses. The specific application may make some characteristics more important than others; for example, a material to be used to shield something from a weak magnetic field would have high initial permeability as its most important criterion. Properties of some important soft materials are listed in Table 13.6b.[16,17] When ferromagnetic metals are used in situations where the magnetic field is time varying, as in a generator or a transformer, so-called *eddy currents* are induced by electric fields prescribed by Faraday's law (Sec. 3.2). The currents are large because the metals have rather high conductivity; the resulting Joule (I^2R) losses can be unacceptable. The currents and resulting losses are minimized by making the cores laminated with the induced current directions perpendicular to the laminations. The losses in metallic ferromagnetic materials become intolerable for radio and microwave frequencies. Ferrites are important because they typically have very low conductivities ($\ll 10^{-4}$ S/m). They are used extensively for purposes such as cores in transformers and filters and antenna rods for frequencies throughout the radio frequency ranges.[18] Several microwave applications utilize an anisotropic property of ferrites; these are discussed in Sec. 13.15.

For the materials discussed here, the permeability as defined by $\mu = B/H$ is not a constant. In solving field problems, however, one is often concerned with small variations of the field about some large average value. If the variations are small enough, any part of the hysteresis loop can be considered a straight line, the slope of which depends upon the point on the loop. The slope is called the *incremental permeability* and is the ratio $\Delta B/\Delta H$.

An effect similar to that discussed for magnetization is found for electric polarization in some materials (e.g., barium titanate). These materials, called *ferroelectric* because their behavior is analogous to that of ferromagnetic materials, exhibit a hysteresis loop in the relationship between the flux density D and the electric field E. As in ferromagnetic materials, a domain structure is found in ferroelectric materials. The details of the interactions between neighboring dipoles are discussed in texts on solid-state physics.[19]

[17] *R. Boll (Ed.),* Soft Magnetic Materials, *Heyden, London/Philadelphia/Rheine, 1979.*
[18] *A. Goldman,* Modern Ferrite Technology, *Van Nostrand Reinhold, New York, 1990.*
[19] *For example, see C. Kittel.*[1]

Table 13.6b
Soft Magnetic Materials

Material	Comment and Percent Composition	Initial Permeability $(\mu_r)_0$	Maximum Permeability $(\mu_r)_{max}$	Coercive Force $\times 10^4$ (A m^{-1})	Saturation Induction (T)
Iron	Commercial (99 Fe)	2×10^2	6×10^3	0.9	2.16
Iron	Pure (99.9 Fe)	2.5×10^4	3.5×10^5	0.01	2.16
Hypersil	97 Fe, 3 Si	9×10^3	4×10^4	0.15	2.01
78 permalloy	78 Ni, 22 Fe	4×10^3	1×10^5	0.05	1.05
Mumetal	18 Fe, 75 Ni, 5 Cu, 2 Cr	2×10^4	1×10^5	0.05	0.75
Supermalloy	15 Fe, 79 Ni, 5 Mo, 0.5 Mn	9×10^4	1×10^6	0.004	0.8
Cryoperm[a]	Usable at cryogenic temperatures	6.5×10^4			

[a]Permeability given for $T = 4.2$ K. See footnote 17.

13.7 Nonlinear Dielectrics: Application in Optics

Most of this text is concerned with linear materials. We have, however, seen in the preceding section that the nonlinear characteristics of ferromagnetic materials must usually be considered. For these, magnetization **M** is a nonlinear function of magnetic field **H**. The polarization **P** of dielectrics may similarly become a nonlinear function of electric field **E** for sufficiently high fields. It is less common to have to consider this nonlinearity than that of ferromagnetic materials, but there is one area in which it is central and has led to a number of useful effects. Because of the high fields of laser beams, nonlinearities in the interaction of materials with optical waves have led to both useful and undesirable effects. We will use this subject of *nonlinear optics* to give the basis for nonlinear polarization, illustrating with applications to heterodyning and harmonic generation. Other important applications such as parametric amplification and oscillation and four-wave mixing to produce conjugate waves (which can be used, for example, to correct wavefront distortion arising from material inhomogeneities[20]) are included in some of the special texts on this subject.[21–23]

A complete theoretical treatment of this subject is complicated by the use, in practice, of anisotropic crystals, in which case the material response is in a direction different from that of the applied field, and directions of propagation of various components can differ. The analysis here avoids those complications while giving the essentials for

[20] *A. Yariv,* IEEE J. Quantum Electronics ***QE-14****, 650 (1978).*
[21] *N. Bloembergen,* Nonlinear Optics, *W. A. Benjamin, New York, 1954.*
[22] *A. Yariv and P. Yeh,* Optical Waves in Crystals, *Chap. 12, Wiley, New York, 1984.*
[23] *H. A. Haus,* Waves and Fields in Optoelectronics, *Chap. 13, Prentice Hall, Englewood Cliffs, NJ, 1984.*

understanding the most important phenomena. With proper interpretation the analysis given below can be adapted to anisotropic crystals.

In Sec. 13.2, we discussed the Lorentz model for the dynamics of the charge cloud in an atom when an oscillating field is applied. For the calculation of the nonlinear polarizability or susceptibility, a modified form of the Lorentz equation is used:

$$\frac{d^2r}{dt^2} + \Gamma\frac{dr}{dt} + \omega_0^2 r - \xi r^2 = -\frac{e}{m}E_{\text{loc}} \tag{1}$$

The nonlinearity becomes significant when the field is large enough to make the displacement r a significant fraction of the radius of the equilibrium electron orbit. Such atomic fields are on the order of 3×10^{10} V/m.[24] One can begin to observe nonlinearities with fields typically 10^{-5} to 10^{-4} of this value so that the perturbation theoretical approach discussed below can be used to calculate r.

We will examine a typical case of interest for applications in which the electric field is the sum of the fields in several waves of different frequencies $E = E(\omega_1) + E(\omega_2) + \cdots$. It is possible to work through the algebra for this case to find expressions for the frequency dependences of the nonlinear polarizations of various orders. The total polarization can be written as

$$P = P_1 + P_2 + \cdots \tag{2}$$

where

$$P_i = -Ner_i \tag{3}$$

in which N is the volume density of atoms, e is the electronic charge, and the displacements r_i are related to the total electric field by

$$r_i = a_i(gE)^i \tag{4}$$

where g is the factor relating the macroscopic field to that acting on the atom. Then the total polarization is

$$\begin{aligned} P &= (-Nea_1g)E + (-Nea_2g^2)E^2 + \cdots \\ &= \varepsilon_0\chi_e E + \varepsilon_0\chi_e^{(2)}E^2 + \cdots \end{aligned} \tag{5}$$

The coefficients a_i and, therefore, the susceptibilities $\chi_e^{(i)}$ are frequency dependent. For example, the form of the frequency dependence of a_1 was given in Eq. 13.2(9). The frequency dependences in the higher-order terms are quite complicated when E is the sum of the fields of several frequencies.

When all frequencies of applied fields are in the optical transmission region of a crystal, it is a good approximation to neglect the frequency dependence of the susceptibility $\chi_e^{(2)}$. The examples treated here need only $\chi_e^{(2)}$, so that P_3, P_4, and so on, may be neglected. Others of the useful processes depend upon $\chi_e^{(3)}$, for example, soliton transmission in fibers, which will be discussed in Chapter 14. For materials having

[24] *N. Bloembergen,* Nonlinear Optics, *p. 7. W. A. Benjamin, New York, 1954.*

inversion symmetry, including isotropic materials, the lowest nonlinear susceptibility is $\chi_e^{(3)}$.

For materials in which P_2 is the dominant nonlinear polarization,

$$P_2 = \varepsilon_0 \chi_e^{(2)} E^2 = 2\varepsilon_0 d E^2 \tag{6}$$

where $d = \chi_e^{(2)}/2$ is a common notation for such materials. Let us find the nonlinear polarization when two plane waves with parallel propagation and different frequencies coexist in such a crystal. We write the two waves as[25]

$$\begin{aligned} E_1(z, t) &= E_1 \cos(\omega_1 t - k_1 z) \\ E_2(z, t) &= E_2 \cos(\omega_2 t - k_2 z) \end{aligned} \tag{7}$$

The electric field in (6) is the sum of the fields of the two waves in (7); making the substitution gives

$$\begin{aligned} P_2 = 2\varepsilon_0 d[&E_1^2 \cos^2(\omega_1 t - k_1 z) + E_2^2 \cos^2(\omega_2 t - k_2 z) \\ &+ 2E_1 E_2 \cos(\omega_1 t - k_1 z) \cos(\omega_2 t - k_2 z)] \end{aligned} \tag{8}$$

Use of trigonometric identities on (8) reveals that it contains components at several different frequencies. There are components at the second harmonic of the two applied frequencies:

$$P_{2\omega_1} = d\varepsilon_0 E_1^2 \cos[2(\omega_1 t - k_1 z)] \tag{9}$$

$$P_{2\omega_2} = d\varepsilon_0 E_2^2 \cos[2(\omega_2 t - k_2 z)] \tag{10}$$

Also, there are components at the sum and difference frequencies,

$$P_{\omega_1 + \omega_2} = 2\, d\varepsilon_0 E_1 E_2 \cos[(\omega_1 + \omega_2)t - (k_1 + k_2)z] \tag{11}$$

$$P_{\omega_1 - \omega_2} = 2\, d\varepsilon_0 E_1 E_2 \cos[(\omega_1 - \omega_2)t - (k_1 - k_2)z] \tag{12}$$

and a time-independent term.

To further complicate matters, E_1, E_2, and P may not be in the same direction, in which case the constant d depends upon the relative directions. Moreover, the direction of propagation (z direction) is not necessarily along a crystal axis. All of these complications must be taken into account when choosing a crystal for harmonic generation or frequency shifting.

It is of use to visualize the polarization for a simple case. Consider the situation where $E_2 = 0$; only the constant polarization and that at $2\omega_1$ remain from the nonlinear terms. Figure 13.7 shows the spatial variation of the applied field and the polarization at $2\omega_1$. The polarization has a phase constant of $2k_1$. For all parts of this pattern of dipoles to produce fields that add constructively, the phase constant of these fields, $k(2\omega_1) = 2k(\omega_1) = 2n(\omega_1)\omega_1/c$. Since $k(2\omega_1) = n(2\omega_1)2\omega_1/c$,

$$n(2\omega_1) = n(\omega_1) \tag{13}$$

[25] *Note that if complex phasors are used, full equivalence to (7) must be included,* $E_i e^{j\omega t} + E_i^* e^{-j\omega t}$ *since real and imaginary parts do not remain separated in nonlinear problems. See Appendix 4.*

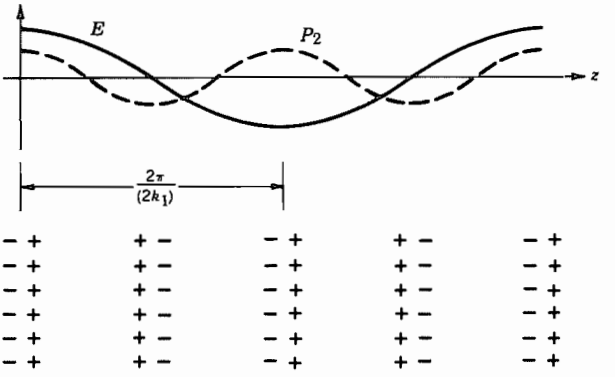

FIG. 13.7 Nonlinear polarization resulting from a single applied electric field of wave number k_1.

The same phase synchronism condition is true for the other components when both sources are present. For example, for $P_{\omega_1-\omega_2}$, the phase constant of the polarization is $k_1 - k_2$. Then for there to be constructive interference so that a net output is created, the index of refraction at $\omega_1 - \omega_2$ must equal that at ω_1:

$$n(\omega_1 - \omega_2) = n(\omega_1) \tag{14}$$

The technique for getting contributions to add constructively is called *phase matching*; it requires control of the index of refraction at the frequencies of the fields involved in generating a particular polarization component and at the frequency of the polarization source term. It is generally possible to do this with only one nonlinear interaction process at a time. Techniques for accomplishing this include temperature control and crystal orientation.

Two important applications are illustrated by the components discussed above. Efficient generation of the second harmonic makes possible signal sources in frequency ranges not otherwise accessible. For example, useful amounts of light at $\lambda_0 = 0.53\ \mu$m can be generated by focusing an intense laser beam from a Nd^{3+}:YAG laser at $\lambda_0 = 1.06\ \mu$m on a crystal of $BaNaNb_5O_{15}$, which has a relatively large value of the constant d. Also, nonlinear polarization can be used to frequency-shift a signal say, at ω_3 to a frequency for which more convenient detectors may be available. Suitable choice of ω_1 can give the desired difference frequency component at $\omega_2 = \omega_3 - \omega_1$.

Power in nonlinear effects of this kind (lossless) is governed by the important Manley–Rowe relations.[26] The changes in power ΔW_{Ti} in the various components are related by

$$\frac{\Delta W_{T1}}{\omega_1} = \frac{\Delta W_{T2}}{\omega_2} = -\frac{\Delta W_{T3}}{\omega_3} \tag{15}$$

where $\omega_3 = \omega_1 + \omega_2$. For example, these show that in the sum-frequency generation, the two source waves at ω_1 and ω_2 lose power to the sum in amounts related to their relative frequencies.

[26] *A. Yariv,* Quantum Electronics, *3rd ed., Sec. 17.0, Wiley, New York, 1989.*

Anisotropic Media

13.8 Representation of Anisotropic Dielectric Crystals

The materials studied up to this point have been representable by scalar permittivities and permeabilities, which may be frequency dependent and nonlinear. In a number of technically important materials, responses to fields with different orientations can differ; that is, they are anisotropic. This anisotropy may be in the response either to the electric field or to the magnetic field. In the former case, the permittivity must be represented by a matrix, an array of nine scalar quantities that may be frequency-dependent and/or nonlinear. The anisotropy in the magnetic field response is represented by a matrix permeability.[27] It is rare that both the permeability and the permittivity are significantly anisotropic and we will not consider that possibility here.[28] We first treat anisotropic dielectric crystals, then ferrites and plasmas having anisotropy caused by the application of a constant magnetic field. In addition to analyzing the representation of these anisotropic materials, we investigate the types of waves that can exist in the various media and comment on applications.

The relation between **D** and **E** for an anisotropic dielectric is given by[29]

$$\begin{aligned} D_x &= \varepsilon_{11}E_x + \varepsilon_{12}E_y + \varepsilon_{13}E_z \\ D_y &= \varepsilon_{21}E_x + \varepsilon_{22}E_y + \varepsilon_{23}E_z \\ D_z &= \varepsilon_{31}E_x + \varepsilon_{32}E_y + \varepsilon_{33}E_z \end{aligned} \tag{1}$$

or, in matrix form,

$$\begin{bmatrix} D_x \\ D_y \\ D_z \end{bmatrix} = \begin{bmatrix} \varepsilon_{11} & \varepsilon_{12} & \varepsilon_{13} \\ \varepsilon_{21} & \varepsilon_{22} & \varepsilon_{23} \\ \varepsilon_{31} & \varepsilon_{32} & \varepsilon_{33} \end{bmatrix} \begin{bmatrix} E_x \\ E_y \\ E_z \end{bmatrix} \tag{2}$$

or, still more compactly,

$$[D] = [\varepsilon][E] \tag{3}$$

[27] *It is sometimes convenient to use either* tensor *or* dyadic *representation for the anisotropic permittivity and permeability, for example, in equations involving curl operators. For an introduction to dyadic notation, see R. E. Collin,* Field Theory of Guided Waves, *2nd ed., pp. 801–803, IEEE Press, Piscataway, NJ, 1991, and for tensors see J. A. Stratton,* Electromagnetic Theory, *Sec. 1.20, McGraw-Hill, New York, 1941. For our purposes, the more common matrix representation suffices.*

[28] *A treatment of the case where both permittivity and permeability are significantly anisotropic, as occurs in yttrium–iron–garnet (YIG) at infrared frequencies, is given by E. E. Bergmann,* Bell System Tech. J. ***61****, 935 (1983).*

[29] *More details may be found in M. Born and E. Wolf,* Principles of Optics, *6th ed., Chap. XIV, Pergamon Press, New York, 1980. See also A. Yariv and P. Yeh,* Optical Waves in Crystals, *Chaps. 4 and 5, Wiley, New York, 1984; and H. A. Haus,* Waves and Fields in Optoelectronics, *Chap. 11, Prentice Hall, Englewood Cliffs, NJ, 1984.*

It can be shown that for physically real materials, the permittivity operator (represented here by a matrix) is Hermitian, a property defined by

$$\varepsilon_{ij} = \varepsilon_{ji}^{*} \tag{4}$$

We will first consider loss-free crystals so (4) implies real and symmetric matrices.[30]

It is a property of symmetric matrices that they can be diagonalized by a rotation of coordinates so that (1) reduces to

$$D_x = \varepsilon_{11}E_x; \qquad D_y = \varepsilon_{22}E_y; \qquad D_z = \varepsilon_{33}E_z \tag{5}$$

where ε_{11}, ε_{22}, and ε_{33} are called the *principal permittivities*. The properties of the matrix can be studied with no loss of generality and with considerable algebraic simplification by using the *principal coordinates*, in which the matrix is diagonalized.

Now we will introduce a geometrical formalism for describing crystal permittivity that aids in the understanding of wave propagation. The electric energy density can be found in the same form, Eq. 1.21(7), as for the isotropic case[31]:

$$U = \tfrac{1}{2}\mathbf{D} \cdot \mathbf{E} \tag{6}$$

Therefore, from (5) and (6):

$$U = \frac{1}{2}\left(\frac{D_x^2}{\varepsilon_{11}} + \frac{D_y^2}{\varepsilon_{22}} + \frac{D_z^2}{\varepsilon_{33}}\right) \tag{7}$$

If we define quantities X, Y, and Z measured along the three principal spatial axes by

$$X = \frac{D_x}{\sqrt{2\varepsilon_0 U}}; \qquad Y = \frac{D_y}{\sqrt{2\varepsilon_0 U}}; \qquad Z = \frac{D_z}{\sqrt{2\varepsilon_0 U}} \tag{8}$$

then (7) becomes

$$\frac{X^2}{(\varepsilon_{11}/\varepsilon_0)} + \frac{Y^2}{(\varepsilon_{22}/\varepsilon_0)} + \frac{Z^2}{(\varepsilon_{33}/\varepsilon_0)} = 1 \tag{9}$$

This is the equation of an ellipsoid; it is known as the *index ellipsoid* (also called the *index of wave normals*, *optical indicatrix*, or *reciprocal ellipsoid*) and has as its semiaxes the square roots of the relative permittivities in the three principal directions, as shown in Fig. 13.8. The name *index ellipsoid* derives from the fact that the index of refraction equals the square root of relative permittivity when $\mu = \mu_0$.

The shape of the ellipsoid depends on the crystalline properties of the materials. Crystals can be divided into three optical classifications. Type I materials have cubic symmetry, for which there are three equivalent directions. In this case $\varepsilon_{11} = \varepsilon_{22} =$

[30] *For magnetically anisotropic real materials, the permeability is Hermitian so that* $\mu_{ij} = \mu_{ji}^{*}$. *For loss-free ferrites and plasmas with applied magnetic field and, to a lesser extent in dielectrics, the* $[\mu]$ *matrices are antisymmetric, so the off-diagonal terms must be imaginary.*

[31] *D. J. Griffiths,* Introduction to Electrodynamics, *2nd ed., p. 185, Prentice Hall, Englewood Cliffs, NJ, 1989.*

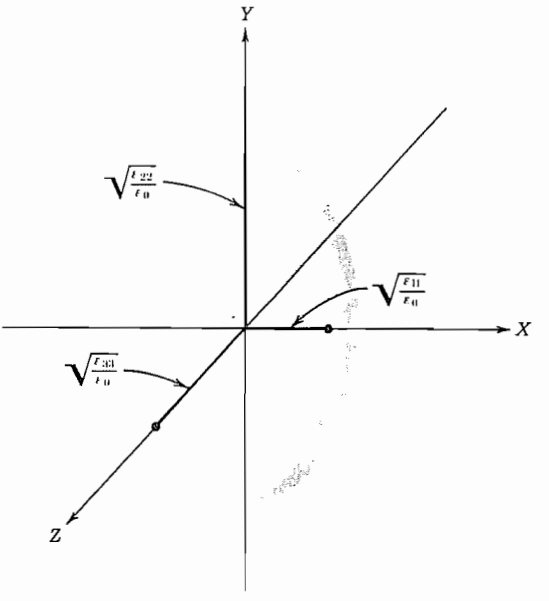

FIG. 13.8 The index ellipsoid.

ε_{33}, the ellipsoid reduces to a sphere, and the properties are isotropic. Silicon, gallium arsenide, and cadmium telluride are examples of cubic crystals. Type II materials include trigonal, tetragonal, and hexagonal crystals, which all have one axis of symmetry. This axis is one of the principal axes of the permittivity ellipsoid. The symmetry of the crystal about this axis requires corresponding symmetry of the ellipsoid. It is, therefore, an ellipsoid of revolution, or spheroid. Crystals of this type are called *uniaxial* and include such important materials as calcium carbonate, quartz, lithium niobate, and cadmium sulfide. Type III or *biaxial* materials are crystals having no axes of symmetry; these are the orthorhombic, monoclinic, and triclinic systems. All three principal axes of the ellipsoid are different, as shown for the general ellipsoid in Fig. 13.8.

13.9 Plane-Wave Propagation in Anisotropic Crystals

The general properties of plane-wave propagation in anisotropic crystals are developed in this section. We will see that **E**, **D**, the wave normal $\boldsymbol{\beta}$, and the Poynting vector **P** all lie in a common plane perpendicular to **H**. It is then shown that there are always two linearly polarized waves (except in certain degenerate situations) with orthogonal orientations of the **D** vectors for each direction of propagation.

It is convenient to introduce here the expression for a wave with a plane phase front oriented in an arbitrary direction. The physical quantities of the wave may be assumed to vary as $e^{-j\boldsymbol{\beta}\cdot\mathbf{r}}$ where

$$\boldsymbol{\beta} = \hat{\mathbf{x}}\beta_x + \hat{\mathbf{y}}\beta_y + \hat{\mathbf{z}}\beta_z$$

is a vector phase factor and

$$\mathbf{r} = \hat{\mathbf{x}}x + \hat{\mathbf{y}}y + \hat{\mathbf{z}}z \tag{1}$$

is the vector distance from an arbitrary origin. Thus we may write

$$\mathbf{E} = \mathbf{E}e^{-j\boldsymbol{\beta}\cdot\mathbf{r}}; \qquad \mathbf{D} = \mathbf{D}e^{-j\boldsymbol{\beta}\cdot\mathbf{r}}; \qquad \mathbf{H} = \mathbf{H}e^{-j\boldsymbol{\beta}\cdot\mathbf{r}} \tag{2}$$

where the coefficients $\mathbf{E}$, $\mathbf{D}$, and $\mathbf{H}$ are constant complex vectors for the electric field intensity, electric flux density, and magnetic field intensity with all spatial dependence removed. Constant phase surfaces are those for which $\boldsymbol{\beta} \cdot \mathbf{r} = \beta r \cos\theta =$ constant, where θ is the angle between $\boldsymbol{\beta}$ and $\mathbf{r}$. It is evident from Fig. 13.9*a* that the constant phase surfaces are planes.

Let us substitute $\mathbf{D}$ and $\mathbf{H}$ in the form (2) into Maxwell's equation

$$\nabla \times \mathbf{H} = j\omega\mathbf{D}$$

and apply the vector identity

$$\nabla \times (\Phi\mathbf{A}) = \nabla\Phi \times \mathbf{A} + \Phi\nabla \times \mathbf{A}$$

where Φ is a scalar and $\mathbf{A}$ is an arbitrary vector. The result is

$$(-j\boldsymbol{\beta} \times \mathbf{H})e^{-j\boldsymbol{\beta}\cdot\mathbf{r}} + e^{-j\boldsymbol{\beta}\cdot\mathbf{r}}\nabla \times \mathbf{H} = j\omega\mathbf{D}e^{-j\boldsymbol{\beta}\cdot\mathbf{r}}$$

Noting that $\nabla \times \mathbf{H} = 0$ since $\mathbf{H}$ is spatially invariant, we obtain

$$-\boldsymbol{\beta} \times \mathbf{H} = \omega\mathbf{D} \tag{3}$$

Application of the same operations to the other of Maxwell's curl equations, $\nabla \times \mathbf{E} = -j\omega\mu\mathbf{H}$, yields

$$\boldsymbol{\beta} \times \mathbf{E} = \omega\mu\mathbf{H} \tag{4}$$

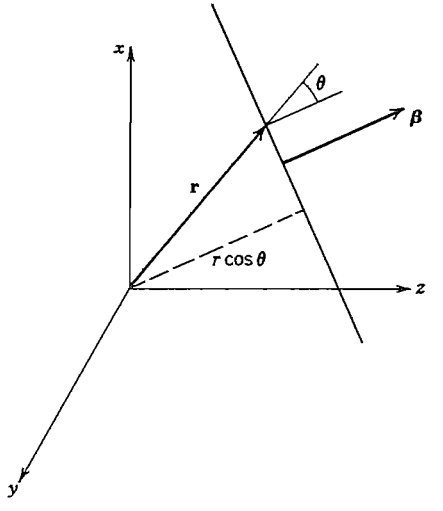

FIG. 13.9*a* Coordinates for a plane wave propagating in an arbitrary direction $\boldsymbol{\beta}$.

Since the vector product is normal to both terms in the product, (3) shows that $\boldsymbol{\beta}$ is perpendicular to $\mathbf{D}$. Similarly, (4) shows that $\boldsymbol{\beta}$ is also normal to $\mathbf{H}$. Therefore $\boldsymbol{\beta}$ is normal to the direction defined by $\mathbf{D}$ and $\mathbf{H}$, which means that constant phase surfaces contain $\mathbf{D}$ and $\mathbf{H}$.

Another important direction of wave propagation is the direction of power flow. This is defined by the Poynting vector

$$\mathbf{P} = \mathbf{E} \times \mathbf{H} \tag{5}$$

In optics the unit vector in the direction of $\mathbf{P}$ is called the *ray vector*.

We see from (3)–(5) that $\mathbf{D}$, $\mathbf{E}$, $\boldsymbol{\beta}$, and $\mathbf{P}$ all lie in the plane perpendicular to $\mathbf{H}$. It is also seen that the ray, or power flow, direction is different from that of the wave normal; the angle separating them is that between $\mathbf{E}$ and $\mathbf{D}$, as seen in Fig. 13.9*b* where $\mathbf{H}$ is normal to the page.

Let us now derive the *Fresnel equation of wave normals* with which it is possible to make some important conclusions about the nature of the allowed waves. Combining (3) and (4) gives

$$\mathbf{D} = -\frac{n^2}{c^2\mu}[\hat{\mathbf{b}} \times (\hat{\mathbf{b}} \times \mathbf{E})] \tag{6}$$

where $\hat{\mathbf{b}}$ is the unit vector in the direction of $\boldsymbol{\beta}$, c is the velocity of light in vacuum, and n is the unknown index of refraction c/v_p in the direction of propagation defined by $\hat{\mathbf{b}}$. Using a vector identity, (6) can be converted to the form

$$\mathbf{D} = \frac{n^2}{c^2\mu}[\mathbf{E} - \hat{\mathbf{b}}(\hat{\mathbf{b}} \cdot \mathbf{E})] \tag{7}$$

Considering the field components lying along the principal axes of the index ellipsoid to simplify the analysis (without any loss of generality) and using Eqs. 13.8(5), (7) becomes

$$\begin{aligned} c^2\mu\varepsilon_{11}E_x &= n^2[E_x - b_x(\hat{\mathbf{b}} \cdot \mathbf{E})] \\ c^2\mu\varepsilon_{22}E_y &= n^2[E_y - b_y(\hat{\mathbf{b}} \cdot \mathbf{E})] \\ c^2\mu\varepsilon_{33}E_z &= n^2[E_z - b_z(\hat{\mathbf{b}} \cdot \mathbf{E})] \end{aligned} \tag{8}$$

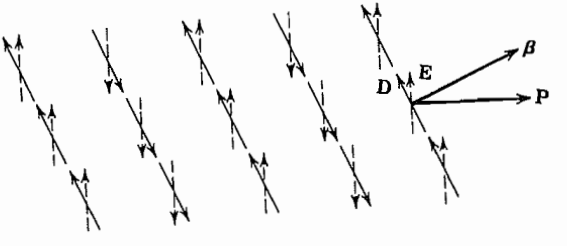

FIG. 13.9*b* Relative directions of the field vectors $\mathbf{D}$ and $\mathbf{E}$, the wave vector $\boldsymbol{\beta}$, and the Poynting vector $\mathbf{P}$ in an anisotropic crystal. Magnetic field is normal to the plane of the other vectors.

Solving any one of the equations (8) gives

$$E_k = \frac{n^2 b_k(\hat{\mathbf{b}} \cdot \mathbf{E})}{n^2 - c^2\mu\varepsilon_{ii}} \tag{9}$$

where $k = x, y,$ or z and i is the corresponding value 1, 2, or 3. Multiplying E_k by b_k, summing the three expressions $b_k E_k$, and dividing by $\hat{\mathbf{b}} \cdot \mathbf{E}$ give

$$\frac{b_x^2}{n^2 - c^2\mu\varepsilon_{11}} + \frac{b_y^2}{n^2 - c^2\mu\varepsilon_{22}} + \frac{b_z^2}{n^2 - c^2\mu\varepsilon_{33}} = \frac{1}{n^2} \tag{10}$$

If we define the principal velocities of propagation by

$$v_x = \frac{1}{\sqrt{\mu\varepsilon_{11}}}, \qquad v_y = \frac{1}{\sqrt{\mu\varepsilon_{22}}}, \qquad v_z = \frac{1}{\sqrt{\mu\varepsilon_{33}}} \tag{11}$$

Then, substituting (11) and $n = c/v_p$ in (10) and subtracting $b_x^2 + b_y^2 + b_z^2 = 1$ from both sides, we get

$$\frac{b_x^2}{v_p^2 - v_x^2} + \frac{b_y^2}{v_p^2 - v_y^2} + \frac{b_z^2}{v_p^2 - v_z^2} = 0 \tag{12}$$

Also (9) can be converted using $n = c/v_p$ and (11) to

$$E_k = \frac{v_k^2}{v_k^2 - v_p^2} b_k(\hat{\mathbf{b}} \cdot \mathbf{E}) \tag{13}$$

Equation (12) is *Fresnel's equation of wave normals*. It is easily seen to be quadratic in v_p^2. Therefore, for each set (b_x, b_y, b_z) that defines the direction of propagation there are two values of phase velocity.

Using (13) for each value of phase velocity, we can find E_x, E_y, and E_z and, therefore, their ratios, which define the direction of $\mathbf{E}$ corresponding to that of v_p. Likewise, the direction of $\mathbf{D}$ for each value of v_p can be found from $\mathbf{E}$ using the relations in Eqs. 13.8(5). If this procedure is carried through, one finds that the ratios of the components of both $\mathbf{D}$ and $\mathbf{E}$ are real, which signals that the two waves are linearly polarized.

There is a helpful construction that can be used to give the phase velocities for an arbitrary direction of propagation.[32] It can also be used to prove that the $\mathbf{D}$ vectors of the two waves are mutually perpendicular and to determine their directions. A plane passed through the center of the index ellipsoid is oriented so its normal lies in the direction of the wave vector. The ellipse formed by the intersection of the plane and the ellipsoid is shown shaded in Fig. 13.9*c*. It can be shown (Prob. 13.9d) that the lengths of the two semiaxes give the indices of refraction (or, equivalently, the phase velocities) of the two waves. The same analysis shows that the flux density vectors $\mathbf{D}$ for the two waves lie along the minor and major axes of the shaded ellipse as shown.

[32] *M. Born and E. Wolf,* Principles of Optics, *6th ed., Sec. 14.2.3. Pergamon Press, New York, 1980.*

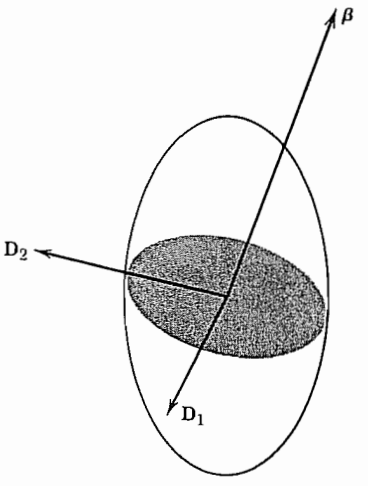

FIG. 13.9c Index ellipsoid with intersecting plane passing through its center. The lengths of the semiaxes of the resulting ellipse give the indices of refraction for the two waves, and the flux density vectors lie along the semiaxes.

13.10 PLANE-WAVE PROPAGATION IN UNIAXIAL CRYSTALS

It was pointed out in Sec. 13.8 that the index ellipsoid for a uniaxial crystal is an ellipsoid of revolution; its axis of symmetry is called the *optic axis*. The Fresnel equation, Eq. 13.9(12), can be specialized to this case by writing $v_z = v_e$ and $v_x = v_y = v_o$:

$$(v_p^2 - v_o^2)[(b_x^2 + b_y^2)(v_p^2 - v_e^2) + b_z^2(v_p^2 - v_o^2)] = 0 \tag{1}$$

If θ is the angle between $\boldsymbol{\beta}$ and the z axis, we can write

$$b_x^2 + b_y^2 = \sin^2\theta; \qquad b_z^2 = \cos^2\theta \tag{2}$$

With (2), the Fresnel equation (1) can be expressed as

$$(v_p^2 - v_o^2)[(v_p^2 - v_e^2)\sin^2\theta + (v_p^2 - v_o^2)\cos^2\theta] = 0 \tag{3}$$

The two roots of (3) are

$$\begin{aligned} v_{p1}^2 &= v_o^2 \\ v_{p2}^2 &= v_o^2\cos^2\theta + v_e^2\sin^2\theta \end{aligned} \tag{4}$$

Note that one wave propagates like a wave in an isotropic medium in that its phase velocity is independent of the direction of propagation. This is called the *ordinary wave*, which is the reason for the subscript o. The other wave has a phase velocity that depends upon the direction of propagation and is called the *extraordinary wave* (subscript e). The two phase velocities are equal only when $\boldsymbol{\beta}$ is along the optic axis (z), as can be seen from (4) with $\theta = 0$.

The polarizations of the flux density vectors of the two waves are along the principal axes of the intersection ellipse in Fig. 13.10*a*. Since the ellipsoid is axially symmetric for the uniaxial case being considered now, the minor axis of the intersection ellipse is unchanged as the direction of propagation is changed. Therefore, the polarization with **D** along the minor axis is that of the ordinary wave and the index measured along that axis corresponds to the velocity v_o. Power flow P_o is parallel to $\boldsymbol{\beta}$ for the ordinary wave as predicted by Eqs. 13.9(3) and 13.9(5) since **D** and **E** are in the same direction ($\mathbf{D} = \hat{\mathbf{y}}D_y = \hat{\mathbf{y}}\varepsilon_{22}E_y$). The extraordinary wave has $\mathbf{D}_e$ along the major axis of the intersection ellipse. Since the angle between $\boldsymbol{\beta}$ and **P** is the same as that between **D** and **E**, we can find the angle between the ray and wave-vector directions by using the permittivities. It is seen in Fig. 13.10*a* that the angle θ between $\boldsymbol{\beta}$ and the z axis is the same as that between $\mathbf{D}_e$ and the x axis so that $\theta = \tan^{-1}(D_z/D_x)$. The **E** vector lies in the plane of $\mathbf{D}_e$, $\boldsymbol{\beta}$, and the z axis (called the *principal section*) and its angle θ' from the x axis is the same as that between **P** and the z axis. Therefore,

$$\tan\theta' = \frac{E_z}{E_x} = \frac{\varepsilon_o D_z}{\varepsilon_e D_x} = \frac{\varepsilon_o}{\varepsilon_e}\tan\theta \tag{5}$$

where $\varepsilon_o = \varepsilon_{11} = \varepsilon_{22}$ and $\varepsilon_e = \varepsilon_{33}$.

Although the details of reflection and refraction of waves at surfaces of anisotropic materials can become quite complicated, the principles are straightforward. Tangential components of **E** and **H** remain continuous across the boundary. Consider, for example, a crystal cut at an angle oblique to the optic axis, as shown in Fig. 13.10*b*. The y axis is the outward normal to the page. It is assumed that the incident plane wave has electric field vectors both in the plane of the page and normal to it. The situation inside the crystal is described by the index ellipsoid in Fig. 13.10*a*. As we saw from Eq. 13.9(3), the **D** vectors lie in the planes of the phase fronts and therefore must lie in the plane of

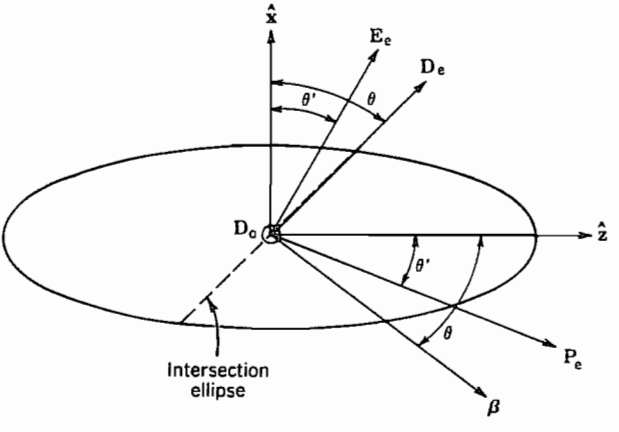

FIG. 13.10*a* Index ellipsoid for a uniaxial crystal with propagation oblique to the optic axis. The intersection ellipse contains the broken line along $\mathbf{D}_e$ and also the $\mathbf{D}_o$ vector normal to the page.

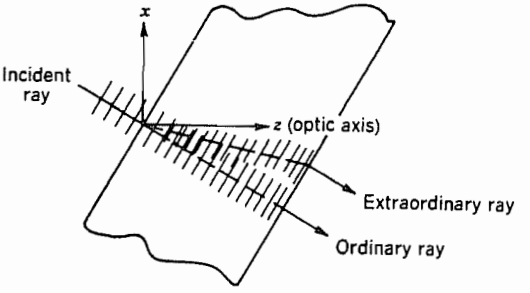

FIG. 13.10*b* Excitation of ordinary and extraordinary waves in a uniaxial crystal with parallel surfaces cut at an angle oblique to the optic axis.

the surface of the crystal since the incoming wave has constant phase on that surface. The dashed line across the ellipsoid in Fig. 13.10*a* is the edge of the intersection ellipse. The flux density $\mathbf{D}_o$ of the ordinary wave is in the y direction out of the page, and $\mathbf{D}_e$ of the extraordinary wave lies in the plane of the page on the major axis of the intersection ellipse. We see from (5) that $\theta' < \theta$ for the ellipsoid illustrated since $\varepsilon_e > \varepsilon_o$. The path of the ray in real space, corresponding to the $\mathbf{P}_e$ direction in the ellipsoid, is shown in Fig. 13.10*b*. Note that β is the same for the two waves, so the phase fronts are parallel even though the extraordinary ray follows a different path from the ordinary ray. The splitting of the refracted wave is called *double refraction* or *birefringence*. The two rays are again parallel after emergence from the planar slab. This is because the continuity conditions depend upon the phase variations along the surface and these are zero for both waves. A common experiment shows this effect. A calcium carbonate crystal is placed on a spot on a piece of paper and two spots are observed, one from the ordinary wave and one from the extraordinary wave, provided the incident wave is unpolarized. If a polarizer is introduced into the incident beam, it can be rotated to eliminate one or the other of the spots.

13.11 Electro-Optic Effects

For certain materials the permittivity can be changed through application of an electric field. For liquids such as carbon disfulfide and nitrobenzene, and for centrosymmetric solids, the effect is proportional to the square of electric field and is known as the *Kerr effect*. For certain noncentrosymmetric solids,[33] such as lithium niobate and gallium arsenide, the change may be directly proportional to applied electric field and is known

[33] *A. Yariv,* Quantum Electronics, *3rd ed., Sec. 14.1, Wiley, New York, 1989. Also see A. Yariv and P. Yeh,* Optical Waves in Crystals, *Chap. 7, Wiley, New York, 1984; and H. A. Haus,* Waves and Fields in Optoelectronics, *Chap. 12, Prentice Hall, Englewood Cliffs, NJ, 1984.*

as the *Pockels effect*. Both effects are relatively small for practical values of electric field, but the latter especially is important in a number of modulators, switches, and deflectors, so that the remainder of this section is devoted to this linear effect in crystals. Its description becomes annoyingly complicated because each component of the permittivity matrix is affected differently depending upon the orientation of the applied field with respect to the crystal axes.

Although one could describe the electro-optic effect by giving the change in permittivity element ε_{ij} when field component E_k is applied, it is customary to define the effect in terms of the reciprocal matrix. Define the matrix

$$\left[\frac{1}{n^2}\right] = \left[\frac{\varepsilon}{\varepsilon_0}\right]^{-1} \tag{1}$$

Then if electric field is applied, the change in an element of this matrix is

$$\Delta\left(\frac{1}{n^2}\right)_{ij} = \sum_{k=1}^{3} r_{ijk} E_k \tag{2}$$

where i, j, k each range over the three spatial coordinates (1, 2, 3 denote x, y, z, respectively). It is also usual to take advantage of the symmetry of the matrices $[\varepsilon]$ and hence $[1/n^2]$ to utilize a contracted notation, $11 \rightarrow 1$, $22 \rightarrow 2$, $33 \rightarrow 3$, $23 = 32 \rightarrow 4$, $13 = 31 \rightarrow 5$, $12 = 21 \rightarrow 6$, so that (2) may be written

$$\Delta\left(\frac{1}{n^2}\right)_p = \sum_{k=1}^{3} r_{pk} E_k \tag{3}$$

with k ranging from 1 to 3 and p from 1 to 6. In matrix form,

$$\begin{bmatrix} \Delta\left(\frac{1}{n^2}\right)_1 \\ \Delta\left(\frac{1}{n^2}\right)_2 \\ \Delta\left(\frac{1}{n^2}\right)_3 \\ \Delta\left(\frac{1}{n^2}\right)_4 \\ \Delta\left(\frac{1}{n^2}\right)_5 \\ \Delta\left(\frac{1}{n^2}\right)_6 \end{bmatrix} = \begin{bmatrix} r_{11} & r_{12} & r_{13} \\ r_{21} & r_{22} & r_{23} \\ r_{31} & r_{32} & r_{33} \\ r_{41} & r_{42} & r_{43} \\ r_{51} & r_{52} & r_{53} \\ r_{61} & r_{62} & r_{63} \end{bmatrix} \begin{bmatrix} E_1 \\ E_2 \\ E_3 \end{bmatrix} \tag{4}$$

Values of r_{pk} for a few crystals are given in Table 13.11.

Table 13.11
Electro-optic Properties

Material	$n_o(\lambda_0 = 550\ \text{nm})$	$n_e(\lambda_0 = 550\ \text{nm})$	r_{pk} in units of 10^{-12} m/V
KDP	1.51	1.47	$r_{41} = 8.6$
(KH_2PO_4)			$r_{63} = 10.6$
GaAs(10.6 μm)	3.34		$r_{41} = 1.6$
$LiNbO_3$	2.29	2.20	$r_{33} = 30.8$
			$r_{13} = 8.6$
			$r_{22} = 3.4$
			$r_{42} = 28$
$BaTiO_3$	2.437	2.365	$r_{33} = 23$
			$r_{13} = 8.0$
			$r_{42} = 820$

From A. Yariv, *Quantum Electronics*, 3rd ed., Table 14.2, Wiley, New York, 1989.

Example 13.11a
ELECTRO-OPTIC PHASE MODULATION

Consider a crystal of lithium niobate as shown in Fig. 13.11*a*, with a wave propagating in the y direction, polarized with electric field in the z direction, and with electrodes placed so that the modulating field is also in the z direction (the optical axis of this crystal). From Table 13.11 we see that applied field $E_z = E_3$, through r_{33}, changes $(1/n^2)_1$ and $(1/n^2)_3$ and no other elements so that the matrix remains diagonalized even after application of the modulating field. (This is not true in general.) The change of $(1/n^2)_1$ cannot affect a wave with $E_z = E_3$ only but the change of $(1/n^2)_3$ is important. From (3),

$$\left(\frac{1}{n^2}\right)_3 = \left(\frac{1}{n_e^2}\right) + r_{33}E_3 \tag{5}$$

where n_e is the index of refraction for extraordinary waves defined in the preceding section. Because of the small value of r_{33},

$$n_3 = \left[\left(\frac{1}{n^2}\right)_3\right]^{-1/2} \approx n_e - \frac{r_{33}n_e^3}{2}E_3 \tag{6}$$

So if the modulating field is

$$E_3 = E_m \cos \omega_m t \tag{7}$$

the phase shift after propagating distance l is

$$\phi(l, t) = \frac{\omega l}{c} n_3 = \frac{\omega l}{c} n_e + \Delta\phi_m \cos \omega_m t \tag{8}$$

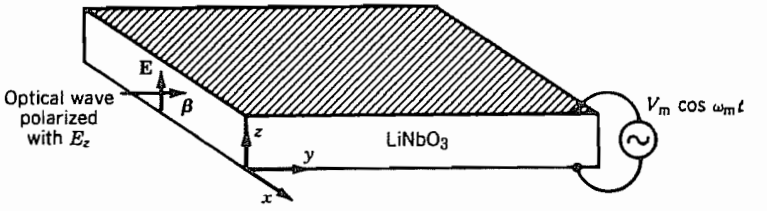

FIG. 13.11*a* Electro-optic phase modulation in $LiNbO_3$ crystal.

where the *modulation index* $\Delta\phi_m$ is

$$\Delta\phi_m = -\frac{\omega l r_{33} n_e^3 E_m}{2c} \tag{9}$$

To make this equal to π (a useful value for the applications to be discussed next) for a signal with free-space wavelength $\lambda_0 = 550$ nm with $l = 1$ cm, E_m would need to be 1.68×10^5 V/m. Although a high field, the required applied voltages are reasonable in thin crystals or thin-film modulators using the optical guiding described in Sec.14.7.

Example 13.11b
CONVERSION OF PHASE MODULATION TO AMPLITUDE MODULATION BY INTERFEROMETRY

Although phase modulation may be used directly for some purposes, it is often desirable to convert this to amplitude modulation. One of the simplest methods is by means of a Mach–Zehnder interferometer sketched in Fig. 13.11*b*.[34] An optical wave is divided

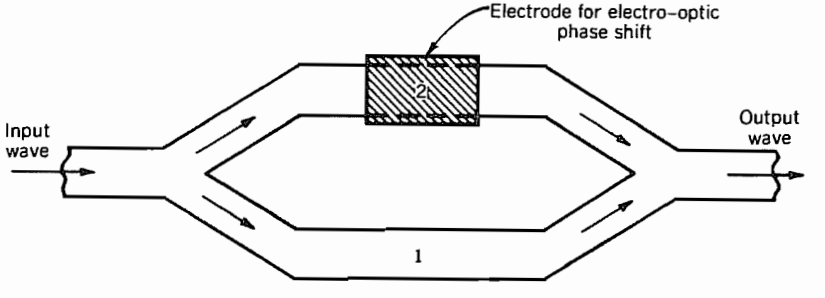

FIG. 13.11*b* Top view of optical waveguide Mach–Zehnder interferometer for converting electro-optic phase modulation to amplitude modulation.

[34] *B. E. A. Saleh and M. C. Teich,* Fundamentals of Photonics, *p. 704, Wiley, New York, 1991.*

into two equal parts by the first Y junction, electro-optic phase shift is introduced into one arm, and then the two waves are combined in the second Y junction. With zero phase shift the two add, with π phase shift they cancel, and with intermediate phases there is a value in between so that 100% modulation is possible. The device is thus also useful as a switch.

Example 13.11c

CONVERSION OF PHASE MODULATION TO AMPLITUDE MODULATION BY POLARIZATION SHIFTS

A somewhat more complicated case is that in which phase shifts are converted to a change in direction of polarization, and this in turn is converted to amplitude modulation through use of an analyzer. It is the classic electro-optic modulator, and also illustrates that new principal axes are in general required after application of the electric field. A sketch of the arrangement is shown in Fig. 13.11*c*. The crystal used for the example is KDP and the modulating field is applied in the z (i.e., 3) direction, which is also the optic axis and the direction of wave propagation. From Table 13.11 the pertinent electro-optic coefficient is then r_{63}, telling us that application of electric field E_z adds an off-diagonal element $(1/n^2)_6 = (1/n^2)_{12}$ to the matrix. New principal axes x' and y' after application of E_z are rotated by 45 degrees relative to the crystal axes x and y (Prob. 13.11a). For these

$$\frac{1}{n_{x'}^2} = \frac{1}{n_o^2} + r_{63}E_z, \qquad \frac{1}{n_{y'}^2} = \frac{1}{n_o^2} - r_{63}E_z \tag{10}$$

Since $r_{63}E_z$ is small, these lead to

$$n_{x'} \approx n_o - \frac{n_o^3}{2} r_{63}E_z, \qquad n_{y'} \approx n_o + \frac{n_o^3}{2} r_{63}E_z \tag{11}$$

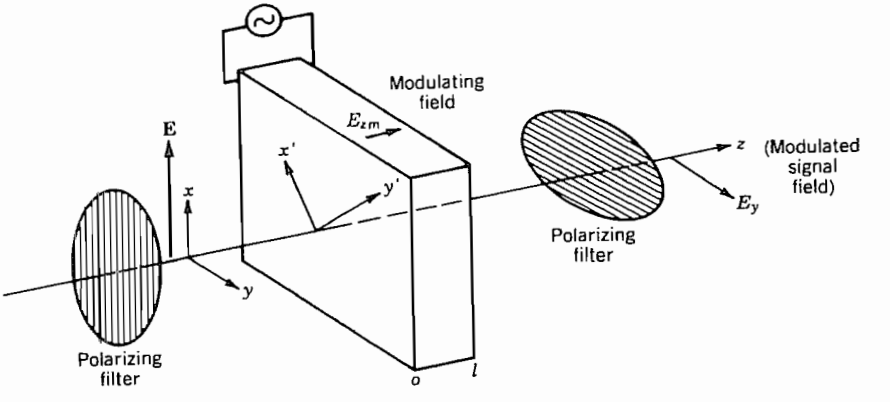

FIG. 13.11c Electro-optic modulator that employs conversion of phase modulation to amplitude modulation.

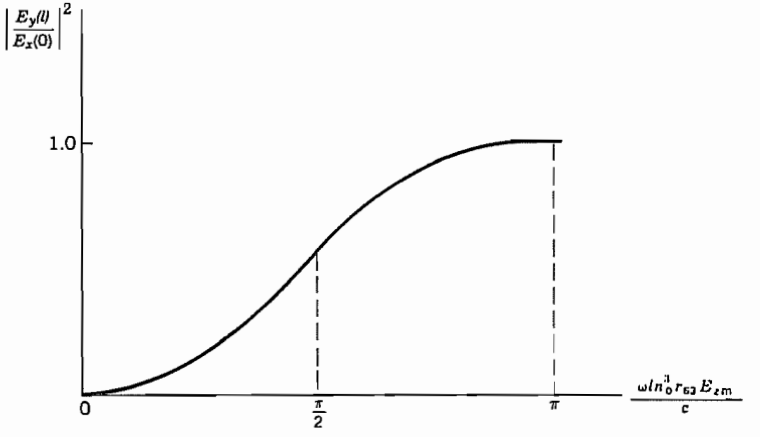

FIG. 13.11*d* Output signal field intensity as a function of modulating field E_z for Fig. 13.11*c*.

The polarizer of Fig. 13.11*c* polarizes with field E_x, which gives equal components in the x' and y' directions:

$$\mathbf{E}(0) = \frac{E_x}{\sqrt{2}}[\hat{\mathbf{x}}' + \hat{\mathbf{y}}'] \tag{12}$$

After propagating distance l,

$$\mathbf{E}(l) = \frac{E_x}{\sqrt{2}} e^{-j(\omega l n_o/c)}[\hat{\mathbf{x}}' e^{j(\omega l n_o^3 r_{63} E_z/2c)} + \hat{\mathbf{y}}' e^{-j(\omega l n_o^3 r_{63} E_z/2c)}] \tag{13}$$

The analyzer selects the y component, which is

$$\begin{aligned} E_y(l) &= \frac{1}{\sqrt{2}}[-E_{x'}(l) + E_{y'}(l)] \\ &= \frac{E_x}{2} e^{-j(\omega l n_o/c)}[-e^{j(\omega l n_o^3 r_{63} E_z/2c)} + e^{-j(\omega l n_o^3 r_{63} E_z/2c)}] \end{aligned} \tag{14}$$

The square of magnitude of this is

$$|E_y(l)|^2 = |E_x|^2 \sin^2 \frac{\omega l n_o^3 r_{63} E_z}{2c} \tag{15}$$

so that it is seen to vary with modulating field E_z according to the curve of Fig. 13.11*d*. A "quarter-wave plate" can be added to shift the operating point with zero modulation to the linear, center part of the curve (Prob. 13.11c). Such a plate produces a phase difference of $\pi/2$ between the two polarizations.

13.12 Permeability Matrix for Ferrites

A group of materials, called ferrites, have the important characteristics of low loss and strong magnetic effects at microwave frequencies. These are solids with a particular type of crystal structure made up of oxygen, iron, and another element which might be lithium, magnesium, zinc, or any of a number of others.[35] The important factors in the study of wave propagation in ferrites are that the losses at microwave frequencies are small, the dielectric constants are relatively high (within a factor of about 2 of $\varepsilon_r = 15$), and anisotropic behavior of permeability results when the ferrite is subjected to a steady magnetic field.

A complete description of the energy state of an atom requires specification of both the orbits and spins of the electrons. In the language of quantum mechanics, there are orbital and spin quantum numbers, both of which must be given to define the energy state of an atom. A strong magnetic moment is associated with the electron spin. In paramagnetic substances these magnetic moments are randomly oriented with respect to those in neighboring atoms, but in ferromagnetic, antiferromagnetic,and ferrimagnetic (ferrite) materials, there exists a strong coupling between spin magnetic moments of neighboring atoms, causing parallel or antiparallel alignment as discussed in Sec. 13.6. We will study the situation in which all the domains are aligned in one direction by a strong applied steady field; the material is saturated. An equation of motion for the spin magnetic moments will be found. By assuming small perturbations of the magnetic field quantities about the large steady values, a permeability matrix for the perturbations will be derived.

The model of the spinning electron used in the derivation is shown diagrammatically in Fig. 13.12*a*. The analogy between the spinning electron and a gyroscope is evident. For any rotating body the rate of change of the angular momentum $\mathbf{J}$ equals the applied torque $\mathbf{T}$:

$$\frac{d\mathbf{J}}{dt} = \mathbf{T} \tag{1}$$

Note as an example the gyroscope shown in Fig. 13.12*b*. The earth's gravitational attraction applies a force or torque to the gyroscope and the angular momentum vector along the axis of the gyroscope rotates slowly about a vertical line through the pivot. This rotation, called *precession*, is at a rate sufficient to conserve the initial angular momentum. For the electron, we relate the magnetic moment $\mathbf{m}$ to the applied torque since

$$\mathbf{m} = \gamma \mathbf{J} \tag{2}$$

where γ is called the *gyromagnetic ratio*.[36] If the electron is considered to be a uniform

[35] *See Goldman*[18] *and R. S. Elliott,* An Introduction to Guided Waves and Microwave Circuits, *Chap. 14, Prentice Hall, Englewood Cliffs, NJ, 1993.*

[36] *The γ of this section is not to be confused with propagation constant, which has the same symbol in other parts of the book.*

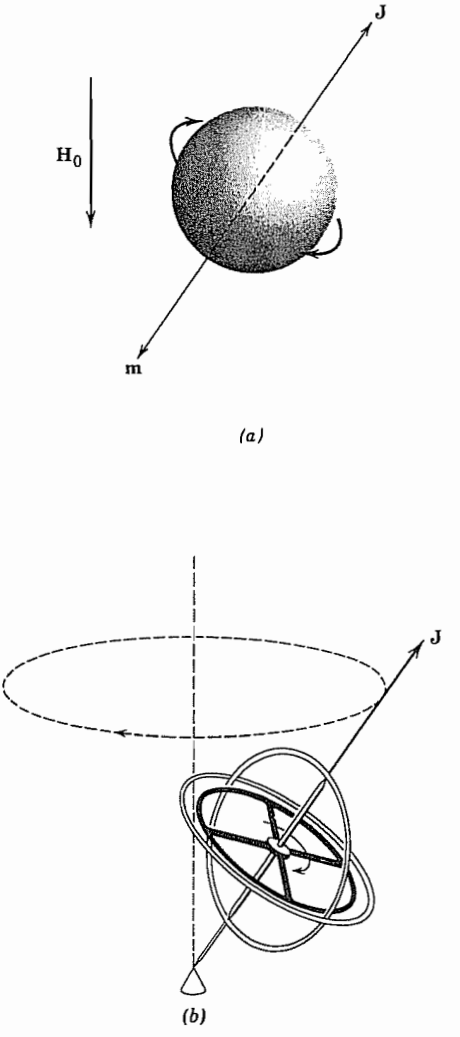

FIG. 13.12 (a) Spherical model of spinning electron in magnetic field. (*b*) Precession of a gyroscope.

charge distribution in a spherical volume and γ is found by classical calculations of $\mathbf{m}$ and $\mathbf{J}$, the result is in error by a factor of almost exactly 2. The correct value of γ, which is approximately -1.759×10^{11} m^2/Wb-s, must be found from quantum mechanics.

The torque resulting from subjecting a magnetic moment $\mathbf{m}$ to a magnetic field $\mathbf{B}_i$ is

$$\mathbf{T} = \mathbf{m} \times \mathbf{B}_i \tag{3}$$

There are also torques resulting from loss mechanisms but these will be neglected here.

We may combine (1) to (3) to get

$$\frac{d\mathbf{m}}{dt} = \gamma(\mathbf{m} \times \mathbf{B}_i) \tag{4}$$

where $\mathbf{B}_i$ is the total field to which the spinning charges are subjected. The total magnetic field acting on a molecule in a magnetic material can be adequately represented by

$$\mathbf{B}_i = \mu_0\mathbf{H} + (\text{constant})(\mathbf{M}) \tag{5}$$

The magnetization vector (or magnetic dipole density) $\mathbf{M}$ is $N_0\mathbf{m}$ where N_0 is the effective number density since all spins in a saturated material act in concert. The magnetic intensity $\mathbf{H}$ is the value averaged over the space of many molecules within the material. The relation between $\mathbf{H}$ and the external applied field depends upon the shape of the ferrite body.

Then combining (4) and (5),

$$\frac{d\mathbf{M}}{dt} = \gamma\mu_0(\mathbf{M} \times \mathbf{H}) \tag{6}$$

Now consider the applied magnetic field in the form of a sum of dc and ac terms:

$$\mathbf{H} = \hat{\mathbf{z}}H_0 + \mathbf{H}_1 e^{j\omega t} \tag{7}$$

The material is saturated, so the magnetization vector must have the form

$$\mathbf{M} = \hat{\mathbf{z}}M_0 + \mathbf{M}_1 e^{j\omega t} \tag{8}$$

where M_0 is the saturation magnetization and $\mathbf{M}_1$ has only x and y components. The expressions (7) and (8) are substituted, in phasor component form, in (6), and all products of ac terms are considered to be negligible compared with products involving one steady term and one alternating term. The result is

$$\begin{aligned} j\omega M_x &= \gamma\mu_0(M_y H_0 - M_0 H_y) \\ j\omega M_y &= \gamma\mu_0(M_0 H_x - M_x H_0) \\ j\omega M_z &= 0 \end{aligned} \tag{9}$$

where the subscript 1 is deleted from the ac term for simplicity. Equations (9) may be solved to give $\mathbf{M}$ in terms of $\mathbf{H}$ and the result substituted in

$$\mathbf{B} = \mu_0(\mathbf{H} + \mathbf{M}) \tag{10}$$

to obtain

$$[B] = [\mu][H] \tag{11}$$

or

$$\begin{bmatrix} B_x \\ B_y \\ B_z \end{bmatrix} = \begin{bmatrix} \mu_{11} & \mu_{12} & 0 \\ \mu_{21} & \mu_{22} & 0 \\ 0 & 0 & \mu_0 \end{bmatrix} \begin{bmatrix} H_x \\ H_y \\ H_z \end{bmatrix} \tag{12}$$

where

$$\mu_{11} = \mu_{22} = \mu_0\left[1 + \frac{\omega_0\omega_M}{\omega_0^2 - \omega^2}\right] \tag{13}$$

$$\mu_{12} = \mu_{21}^* = j\frac{\mu_0\omega\omega_M}{\omega_0^2 - \omega^2} \tag{14}$$

in which

$$\omega_M = -\mu_0\gamma M_0, \quad \omega_0 = -\mu_0\gamma H_0 \tag{15}$$

A resonance occurs at the frequency $\omega_0 = -\gamma\mu_0 H_0 = (e/m)\mu_0 H_0$. Note that the magnetic field H_0 within the ferrite differs from the applied field, as mentioned after (5). The singularity at resonance is suppressed if the mechanisms responsible for damping the precession are considered in the analysis.

13.13 TEM Wave Propagation in Ferrites

Although a complete treatment of practical ferrite devices would require more complicated wave analysis, useful insight into device behavior is given by understanding TEM wave propagation parallel to an applied dc magnetic field. Propagation will be assumed to be in the z direction with variations as $e^{\pm j\beta z}$. Taking the curl of Maxwell's curl $\mathbf{H}$ equation in phasor form, and making use of a vector identity, we have

$$\nabla^2\mathbf{H} - \nabla(\nabla \cdot \mathbf{H}) + \omega^2\varepsilon\mathbf{B} = 0 \tag{1}$$

Since there is no field in the direction of variations (z) and no variation in the direction of the fields (x and y), $\nabla \cdot \mathbf{H} = 0$. The Laplacian reduces to d^2H/dz^2 and we use Eq. 13.12(12) to transform (1) to

$$\frac{d^2}{dz^2}\begin{bmatrix} H_x \\ H_y \\ 0 \end{bmatrix} + \omega^2\varepsilon\begin{bmatrix} \mu_{11} & \mu_{12} & 0 \\ \mu_{21} & \mu_{22} & 0 \\ 0 & 0 & \mu_0 \end{bmatrix}\begin{bmatrix} H_x \\ H_y \\ 0 \end{bmatrix} = 0 \tag{2}$$

For isotropic media wave solutions were taken to be linearly polarized; by suitable orientation of the coordinate system, they might have only one component (e.g., $\mathbf{H} = \hat{\mathbf{x}}H_x$). If we substitute such an assumed form of solution in (2), we find a vector with only an x component in the first term, whereas the vector in the second term has both x and y components. For the sum of two vectors to be zero, their components must individually add to zero. Therefore, the magnitude of the y component must be zero. This is possible only if either μ_{21} or H_x is zero. We know from Sec. 13.12 that μ_{21} is not zero, and if H_x is zero, there is no wave. Thus we must conclude that a linearly polarized wave is not a possible solution; that is, it is not a *normal mode* of propagation

for the medium. We will see that circularly polarized waves are normal modes; media with this property are called *gyrotropic*.

For a clockwise polarized wave (field vectors rotate clockwise as a function of time at a fixed plane in space, looking in the direction of propagation) traveling in the $+z$ direction, the field has the form

$$\mathbf{H}_{+}^{\text{cw}} = H_{+}^{\text{cw}}(\hat{\mathbf{x}} - j\hat{\mathbf{y}}) \tag{3}$$

Substituting (3) in (2) and using Eqs. 13.12(13) and (14), we get the propagation constant

$$\begin{aligned} \beta_{+}^{\text{cw}} &= \omega\sqrt{\varepsilon}(\mu_{11} - j\mu_{12})^{1/2} \\ &= \omega\sqrt{\varepsilon\mu_0}\left(1 + \frac{\omega_M}{\omega_0 - \omega}\right)^{1/2} \end{aligned} \tag{4}$$

The quantity $(\mu_{11} - j\mu_{12})$ that appears in β_{+}^{cw} is shown schematically in Fig. 13.13*a*. The shaded region is a stop band since $(\mu_{11} - j\mu_{12})$ is negative, and β_{+}^{cw} is therefore imaginary. Pumping of the electron spins by the rf magnetic field at the natural precession frequency produces the resonance at ω_0.

For the counterclockwise wave traveling in the $+z$ direction, the magnetic field is

$$\mathbf{H}_{+}^{\text{ccw}} = H_{+}^{\text{ccw}}(\hat{\mathbf{x}} + j\hat{\mathbf{y}}) \tag{5}$$

Then substituting (5) into (2) and using Eqs. 13.12(13) and (14), we find the corresponding propagation constant

$$\begin{aligned} \beta_{+}^{\text{ccw}} &= \omega\sqrt{\varepsilon}(\mu_{11} + j\mu_{12})^{1/2} \\ &= \omega\sqrt{\varepsilon\mu_0}\left(1 + \frac{\omega_M}{\omega_0 + \omega}\right)^{1/2} \end{aligned} \tag{6}$$

The quantity $(\mu_{11} + j\mu_{12})$ is shown schematically in Fig. 13.13*b*.

To complete the set of possible waves, we must consider the two circularly polarized waves propagating in the $-z$ direction. The magnetic fields for the clockwise and counterclockwise waves, respectively, are

$$\mathbf{H}_{-}^{\text{cw}} = H_{-}^{\text{cw}}(\hat{\mathbf{x}} + j\hat{\mathbf{y}}) \tag{7}$$

$$\mathbf{H}_{-}^{\text{ccw}} = H_{-}^{\text{ccw}}(\hat{\mathbf{x}} - j\hat{\mathbf{y}}) \tag{8}$$

Substitution of these forms into the wave equation (2) as was done for the $+z$ traveling waves above yields

$$\beta_{-}^{\text{cw}} = \beta_{+}^{\text{ccw}} = \omega\sqrt{\varepsilon\mu_0}\left(1 + \frac{\omega_M}{\omega_0 + \omega}\right)^{1/2} \tag{9}$$

$$\beta_{-}^{\text{ccw}} = \beta_{+}^{\text{cw}} = \omega\sqrt{\varepsilon\mu_0}\left(1 + \frac{\omega_M}{\omega_0 - \omega}\right)^{1/2} \tag{10}$$

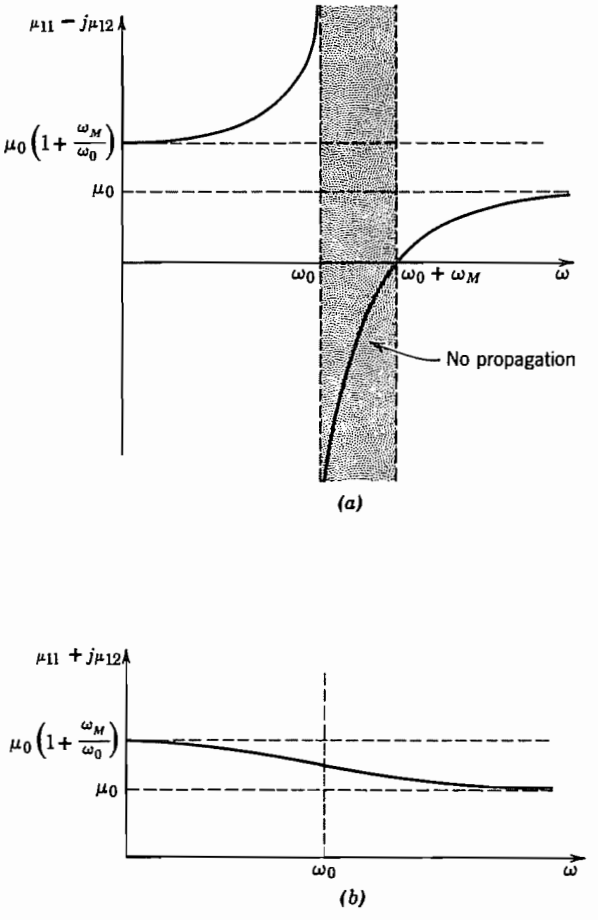

FIG. 13.13 (a) Equivalent permeability for clockwise circularly polarized wave propagating in $+z$ direction. (*b*) Equivalent permeability for counterclockwise circularly polarized wave propagating in $+z$ direction ($\mathbf{H}_0 = \hat{\mathbf{z}}H_0$).

Transmission-Line Analogy We can make use of the transmission-line analogy to solve problems of reflection and transmission with considerable advantage of simplification. To ensure continuity of electric and magnetic fields at a boundary for circularly polarized waves, forward- and reverse-traveling waves having the same absolute direction of rotation must be combined. Thus we sum the fields of the positive-traveling clockwise wave and the negative-traveling counterclockwise wave. The other pair of waves (positive-traveling counterclockwise and negative-traveling clockwise) are handled as a separate problem in the same manner. The two pairs of waves are illustrated in Figs. 13.13*c* and *d*.

Let us consider the pair of waves in Fig. 13.13*c*. The magnetic fields for both of

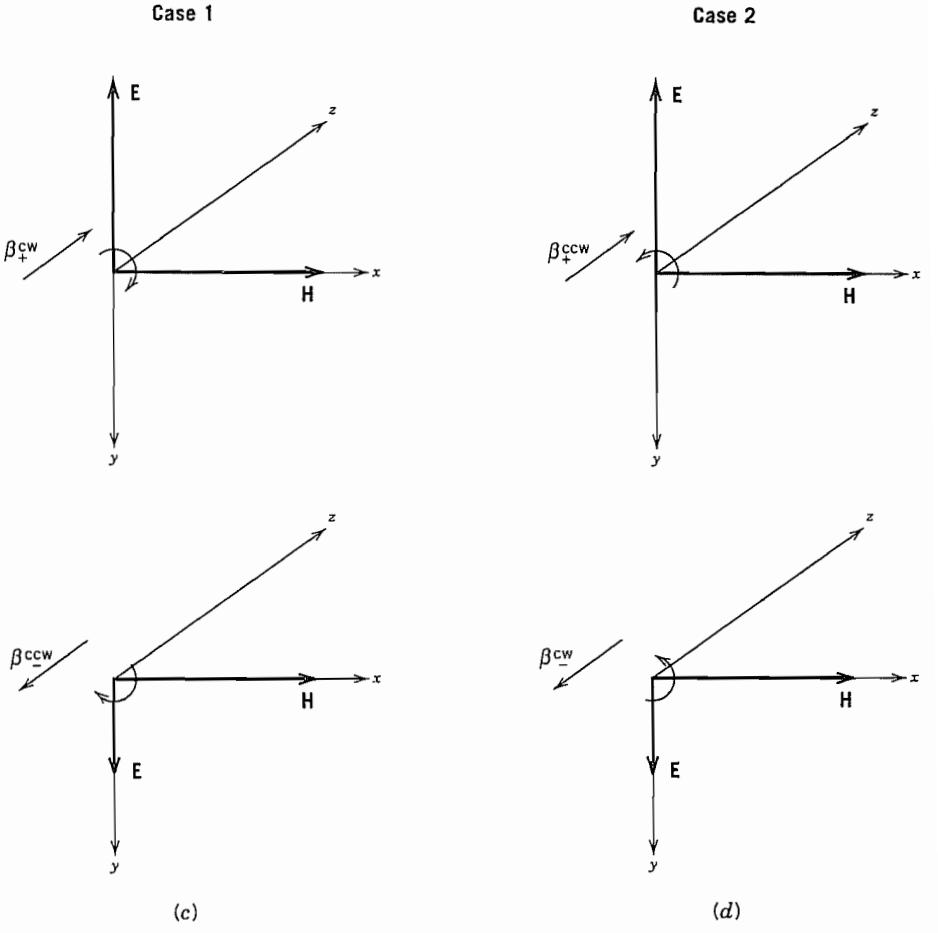

FIG. 13.13 (*c*) Pair of waves having rotation of fields clockwise relative to the $+z$ axis. (*d*) Pair of waves having rotation counterclockwise relative to the $+z$ axis.

these waves have the form in (3). The corresponding electric fields are found by substitution of (3) into Maxwell's curl **H** equation to be

$$\mathbf{E}_+^{cw} = -E_+^{cw}(j\hat{\mathbf{x}} + \hat{\mathbf{y}}) \tag{11}$$

and

$$\mathbf{E}_-^{ccw} = E_-^{ccw}(j\hat{\mathbf{x}} + \hat{\mathbf{y}}) \tag{12}$$

in which the field amplitudes are related by the characteristic wave impedance

$$\eta_1 = \frac{E_+^{cw}}{H_+^{cw}} = \frac{E_-^{ccw}}{H_-^{ccw}} = \frac{\beta_+^{cw}}{\omega\epsilon} = \sqrt{\frac{\mu_0}{\varepsilon}\left(1 + \frac{\omega_M}{\omega_0 - \omega}\right)} \tag{13}$$

where subscript 1 refers to case 1 shown in Fig. 13.13*c*.

The amplitudes of the total fields in case 1 (Fig. 13.13*c*) can then be written as

$$H_1(z) = H_+^{\text{cw}} e^{-j\beta_1 z} + H_-^{\text{ccw}} e^{j\beta_1 z} \tag{14}$$

and

$$E_1(z) = \eta_1 (H_+^{\text{cw}} e^{-j\beta_1 z} - H_-^{\text{ccw}} e^{j\beta_1 z}) \tag{15}$$

where $\beta_1 = \beta_+^{\text{cw}} = \beta_-^{\text{ccw}}$ in (10).

These equations are in the form of the transmission-line equations and the analogy is completed by defining a wave impedance at any plane z as

$$Z_1(z) = \frac{E_1(z)}{H_1(z)} \tag{16}$$

Then all the apparatus of Sec. 6.6 can be adapted to solve problems of reflection and transmission at discontinuities for a circularly polarized wave.

The other pair of waves, those with rotation counterclockwise with respect to the dc magnetic field, as shown in Fig. 13.13*d*, are handled in the same way. The magnetic fields are given by (5) and (7). The electric fields for the two waves and the characteristic wave impedance are found by substituting the magnetic fields into Maxwell's curl **H** equation:

$$\mathbf{E}_+^{\text{ccw}} = E_+^{\text{ccw}}(j\hat{\mathbf{x}} - \hat{\mathbf{y}}), \qquad \mathbf{E}_-^{\text{cw}} = E_-^{\text{cw}}(-j\hat{\mathbf{x}} + \hat{\mathbf{y}}) \tag{17}$$

and

$$\eta_2 = \frac{E_+^{\text{ccw}}}{H_+^{\text{ccw}}} = \frac{E_-^{\text{cw}}}{H_-^{\text{cw}}} = \frac{\beta_2}{\omega\varepsilon} = \sqrt{\frac{\mu_0}{\varepsilon}\left(1 + \frac{\omega_M}{\omega_0 + \omega}\right)} \tag{18}$$

The propagation constant β_2 was given in (9). To use the transmission-line analogy we write expressions for the amplitudes of the total electric field and total magnetic field,

$$H_2(z) = H_+^{\text{ccw}} e^{-j\beta_2 z} + H_-^{\text{cw}} e^{j\beta_2 z} \tag{19}$$

$$E_2(z) = \eta_2 (H_+^{\text{ccw}} e^{-j\beta_2 z} - H_-^{\text{cw}} e^{j\beta_2 z}) \tag{20}$$

with β_2 and η_2 given by (9) and (18), respectively. The wave impedance for this case is

$$Z_2(z) = \frac{E_2(z)}{H_2(z)} \tag{21}$$

An example of the use of these tools in a calculation of the propagation of waves through a layer of ferrite between two isotropic regions with the propagation direction parallel to the dc magnetic field is shown in Fig. 13.13*e*. If the incident wave is linearly polarized, it can be decomposed into two oppositely rotating circularly polarized waves. Each of these can be handled separately since we are considering the media to be linear. The load impedance Z_L at plane 2 for each of type 1 and 2 waves in Figs. 13.13*c* and *d* is the characteristic wave impedance $\eta = \sqrt{\mu_2/\varepsilon_2}$. The impedance transformation Eq. 6.6(10) with k replaced by either β_1 or β_2 gives the wave impedance at plane 1.

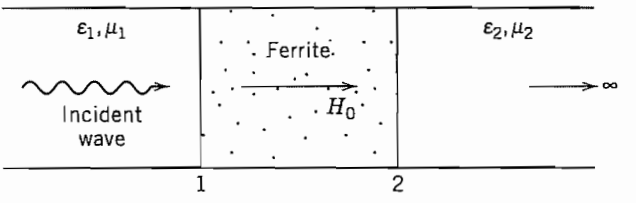

(e)

FIG. 13.13e Example of a problem utilizing transmission-line methods for circularly polarized waves.

Then the reflection coefficient Eq. 6.6(11) gives the relative amplitude of the reflected wave in region 1 for each direction of polarization. Knowing the amplitudes of the incident waves of each circular polarization, the total reflected wave is constructed as the sum of those in the two polarizations.

13.14 FARADAY ROTATION

In this section we shall see how the difference of propagation constants between clockwise and counterclockwise polarized waves can be used to show that a linearly polarized wave is rotated when it passes through a gyrotropic medium. Let us first consider a linearly polarized wave propagating in the $+z$ direction with $\mathbf{H}$ vector in the x direction at the plane $z = 0$ in the ferrite of Sec. 13.13. This field may be decomposed into circularly polarized modes of propagation

$$\mathbf{H}^{cw} = (\hat{\mathbf{x}} - j\hat{\mathbf{y}})\frac{H}{2}e^{-j\beta^{cw}z} \tag{1}$$

and

$$\mathbf{H}^{ccw} = (\hat{\mathbf{x}} + j\hat{\mathbf{y}})\frac{H}{2}e^{-j\beta^{ccw}z} \tag{2}$$

since the sum of (1) and (2) at $z = 0$ is

$$\mathbf{H} = \hat{\mathbf{x}}H$$

This can be thought of as finding magnitudes of the natural modes of the system necessary to match the given boundary condition at $z = 0$.

The field at any other plane, $z =$ constant, is found by adding (1) and (2):

$$\mathbf{H} = \frac{H}{2}[\hat{\mathbf{x}}(e^{-j\beta^{ccw}z} + e^{-j\beta^{cw}z}) + j\hat{\mathbf{y}}(e^{-j\beta^{ccw}z} - e^{-j\beta^{cw}z})] \tag{3}$$

which can be cast into the form

$$\mathbf{H} = He^{-(j/2)(\beta^{cw}+\beta^{ccw})z}\left[\hat{\mathbf{x}}\cos\left(\frac{\beta^{cw}-\beta^{ccw}}{2}\right)z - \hat{\mathbf{y}}\sin\left(\frac{\beta^{cw}-\beta^{ccw}}{2}\right)z\right] \tag{4}$$

The sum wave (4) is seen to have field vectors in a fixed direction at each value of z since there is no phase difference between the x and y components. The direction of the field vector relative to that at $z = 0$ is, as seen in Fig. 13.14, given by

$$\tan \theta = \frac{H_y}{H_x} = -\tan\left(\frac{\beta^{cw} - \beta^{ccw}}{2}\right)z \tag{5}$$

or

$$\theta = \left(\frac{\beta^{ccw} - \beta^{cw}}{2}\right)z \tag{6}$$

The sign of the angle θ is positive for clockwise rotation about the positive z axis. Thus we see that the linearly polarized wave rotates upon passing along the gyrotropic axis (z axis) and has a propagation constant which is the average of those of the clockwise and counterclockwise modes.

It is of special interest to note that the direction of rotation about the positive z axis is the same for waves traveling in the positive and negative z directions. In Sec. 13.15 we see applications of this phenomenon.

The rotation of plane of polarization of an optical wave in passing through a dielectric with an applied magnetic field was first observed by Michael Faraday around 1845; hence, the name *Faraday rotation.* The angle of rotation (6) can be written as

$$\theta = VH_0 l \tag{7}$$

where H_0 is the dc magnetic field strength, l the interaction length, and V a constant known as the *Verdet constant.* This effect is strong in ferrites but is also seen in magnetized plasmas to be discussed in following sections. It is even seen in ordinary dielectrics but θ is small. V is about 0.014 min/Oe-cm in silica at $\lambda_0 = 600$ nm, decreasing at longer wavelengths approximately as λ^{-2}. With the long propagation lengths obtainable with optical fiber guides, useful nonreciprocal devices can nevertheless be made using this effect, but ingenious design is necessary to maintain magnetic field axial in the multiple passes through the magnet.

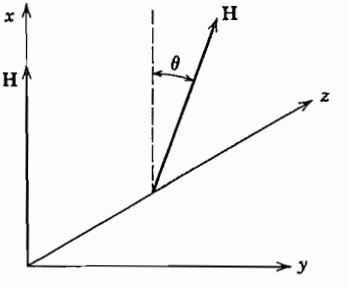

Fig. 13.14 Rotation of a linearly polarized wave in a gyrotropic medium.

13.15 Ferrite Devices

Ferrite devices have found use in microwave applications for both waveguides and striplines. One family operates on the basis of the Faraday effect described in Sec. 13.14 and the others on different principles, to be discussed below, that also depend upon the asymmetry caused by an applied steady magnetic field.

Waveguide Devices The group of devices that employ Faraday rotation take advantage of the fact that the rotation of a linearly polarized wave is in the same direction relative to the direction of the dc magnetic field for both the positive and negative traveling waves. (See Fig. 13.15*a*.) The first and simplest of the microwave devices using the Faraday rotation effect was the *gyrator*,[37] shown in Fig. 13.15*b*. By virtue of a twist of the waveguide, a wave coming from the left is rotated counterclockwise by 90 degrees before reaching the ferrite. The magnetic field and the dimensions of the ferrite are chosen so an additional 90 degrees counterclockwise rotation of the wave takes place in the ferrite region. Thus, the wave progressing toward the right is inverted or, equivalently, shifted in phase by 180 degrees. A wave passing from right to left is rotated by 90 degrees counterclockwise with respect to the direction of the magnetic field, and this is canceled by the rotation in the twisted portion of the guide to the left of the ferrite. The gyrator, therefore, serves to produce a phase shift of 180 degrees in one direction and no shift in the opposite direction.

Another important Faraday rotation device is the *absorption isolator* shown in Fig. 13.15*c*. Here the 45-degree twist to the left of the ferrite rotates the wave coming from the left so that its electric field vectors are perpendicular to the thin resistance card just after the twist. With this orientation, the field suffers a minimum of conduction losses in the card. The field is then rotated back to its original orientation when it passes through the ferrite and leaves the isolator essentially unmodified. A wave traveling to the left is rotated in the ferrite in the same direction relative to the magnetic field as the wave moving to the right and is therefore oriented with its electric field vectors along the resistance card. In this way the wave traveling to the left is appreciably attenuated (typically 30 dB) and the wave moving to the right suffers little loss (usually less than 0.5 dB).

Another application of Faraday rotation is the *circulator* shown in Fig. 13.15*d*. The function of a circulator is to transmit a wave from guide 1 to guide 2, a wave from guide 2 to 3, 3 to 4, and 4 to 1, with all other couplings prohibited. The ferrite rod and magnetic field are chosen to give 45 degree rotation. The TE_{10} mode in guide 1 excites the TE_{11} mode in the circular guide. The symmetry of the TE_{11} circular mode (see Table 8.9) is such that it does not excite propagating waves in guide 3. The right half of the structure is rotated by 45 degrees relative to guides 1 and 3 as seen in Fig. 13.15*d*. A 45-degree rotation of the wave coming from guide 1 places it in the same orientation with respect to 2 and 4 as it had with respect to 1 and 3 so it passes out through guide 2. A TE_{10} wave entering guide 3 excites a TE_{11} mode in the circular guide, but it is

[37] *C. L. Hogan,* Bell System Tech. J. ***31***, *1 (1952).*

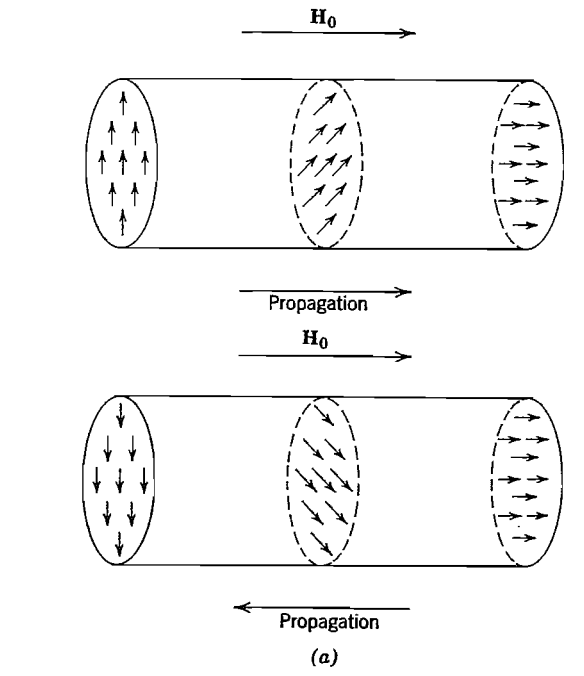

(a)

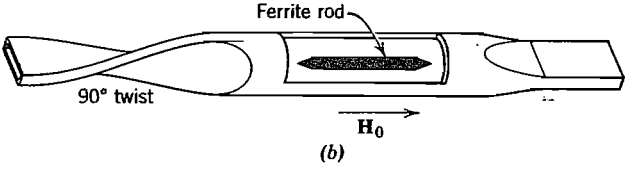

(b)

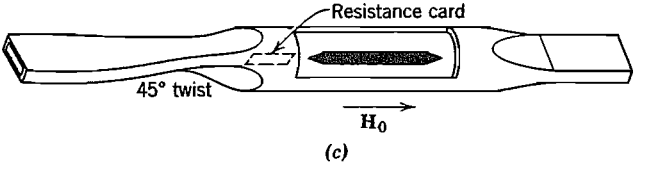

(c)

FIG. 13.15 (*a*) Wave rotation of waves in two directions in magnetized ferrite rod. (*b*) Microwave gyrator. (*c*) Microwave isolator.

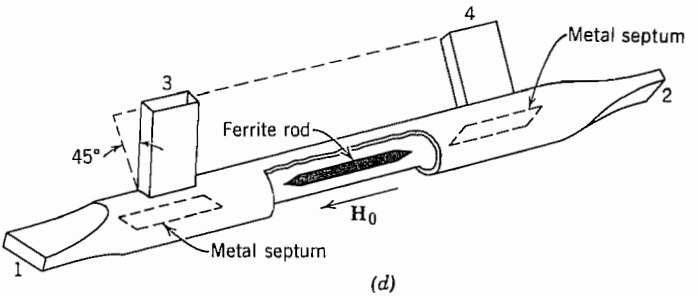

(d)

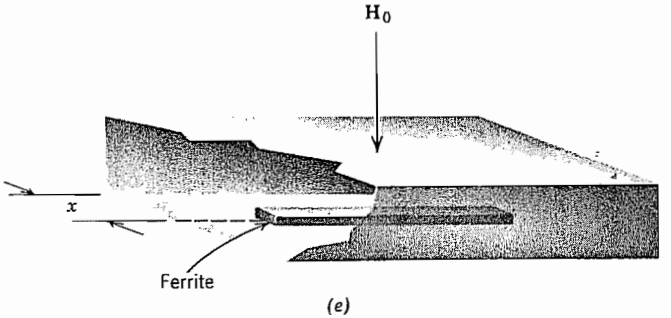

(e)

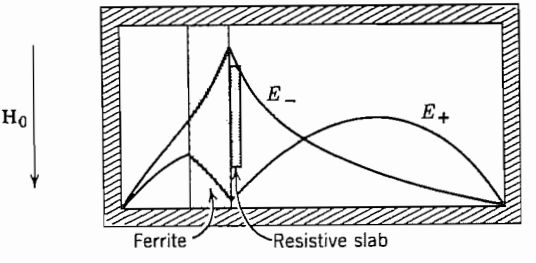

(f)

FIG. 13.15 (*d*) Microwave circulator. (*e*) Ferrite location in resonance isolator. (*f*) Field patterns in field-displacement isolator.

oriented at 90 degrees from the mode excited by a wave from guide 1. It cannot excite propagating modes in 1. When rotated by 45 degrees in the ferrite, the wave is oriented to excite waves in guide 4 but not 2. The analyses of waves entering guides 2 and 4 follow similar reasoning. The metal septums shown in the figure aid in preventing unwanted couplings. The circulator can also be used as a switch or for modulation by controlling the field that magnetizes the ferrite.

The choice of diameter and shape of the ferrite rods used in Faraday rotation devices is made to minimize reflections and maximize power-handling capability while achieving the required rotation with reasonable magnetic fields. Because power is dissipated in the small rod isolated from the walls, a Faraday rotation device is useful only for low power. Some of the following devices have the ferrite connected to the metal wall and can carry higher-power fields.

The functions just described can also be achieved in *resonance* and *field displacement* devices which employ magnetic fields transverse to the guide. Let us consider, for a rectangular waveguide with TE_{10} mode, the rf magnetic fields in the planes perpendicular to the dc magnetization. The vector sum of H_x and H_z of Eqs. 8.8(4) and 8.8(5) is

$$\mathbf{H}_{xz} = \left[\hat{\mathbf{x}} - j\hat{\mathbf{z}}\left(\frac{\lambda}{2a}\right)\frac{Z_{TE}}{\eta}\cot\frac{\pi x}{a}\right]|H|\sin\frac{\pi x}{a} \tag{1}$$

where Z_{TE} is positive for a wave in the $+z$ direction and negative for the reverse wave. It is clear from (1) that at the value of x in the guide such that

$$\left|\left(\frac{\lambda}{2a}\right)\frac{Z_{TE}}{\eta}\cot\frac{\pi x}{a}\right| = 1 \tag{2}$$

the field $\mathbf{H}_{xz}$ is circularly polarized. The direction of polarization depends upon the sign of Z_{TE}.

If a piece of ferrite is placed on the top or bottom of the guide at the value of x given by (2) as shown in Fig. 13.15*e* the precessing electron spin moments will be subjected to a circularly polarized field which either enhances the precession or is very little coupled to it, depending upon the direction of the circular polarization. By appropriate choice of polarity of the dc magnetic field, the direction of spin precession can be made opposite to the direction of rotation of the field vectors of the forward wave. In this case the forward wave is little affected. The backward wave, having an opposite polarization of $\mathbf{H}_{xz}$, pumps the precessing spins and loses energy in the process. This energy is transferred from the electrons to the lattice of the ferrite by microscopic damping mechanisms. If the magnetic field is adjusted to set the resonance frequency equal to the field frequency ($\omega = -\gamma\mu_0 H_0$), the reverse loss is maximum. This device, used as an isolator, requires more dc field than the Faraday rotation isolator described previously, since it must operate at resonance. It has the advantage, however, of allowing convenient cooling of the ferrite. The same mechanism can be used to modulate a wave.

There is a third class of nonreciprocal devices utilizing magnetized ferrites. These also use transverse magnetization but make use of the fact that forward and reverse waves with the ferrite present may have different transverse field distributions. They are called *field displacement* devices. If a slab of ferrite is approximately located and magnetized, an approximate null of electric field can be made to exist at its edge for the forward wave but not for the reverse wave. This is shown schematically in Fig.

13.15*f*. A resistive strip attached to the side of the ferrite then attenuates the reverse wave but does not affect the forward wave. As with Faraday rotation devices, the field displacement scheme is limited to low-power application.

Stripline Devices A device called the *stripline Y-junction circulator* shown in Fig. 13.15*g* can also be used as a switch or isolator. A dc magnetic field is applied normal to the ferrite disks. Operation can be described in terms of standing mode patterns in the disks, similarly to the modes in dielectric resonators (Sec. 10.13).[38,39] The lowest resonant mode is shown in Fig. 13.15*h* for the case with no applied magnetic field; the rf electric field is perpendicular to the plane disk surfaces and magnetic field is transverse. The fields shown are excited by the input in line 1, and lines 2 and 3 receive excitation of magnitude one-half that of the input. In the presence of a magnetic field, the standing pattern comprises two counterrotating field patterns. This new pattern is rotated about the disk axis by an amount that depends upon the magnetic field strength. Figure 13.15*i* shows the pattern rotated to a position in which line 2 receives an excitation equal to the input and line 3 is isolated. The complete symmetry of the device implies that the roles of the lines can be rotated so that excitation in line 2 produces an output in line 3 and nothing in line 1 and similarly for excitation in line 3. See Schloemann's article[40] for practical realization of circulators in microwave and millimeter-wave integrated circuits.

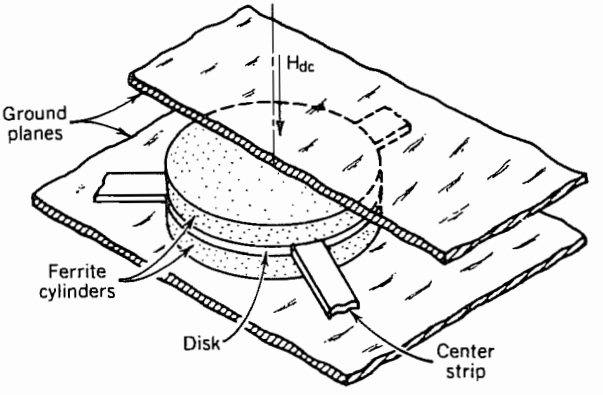

FIG. 13.15 (*g*) Stripline Y-junction circulator. (After Fay and Comstock.[38] © 1965, IEEE.)

[38] *C. E. Fay and R. L. Comstock,* IEEE Trans. Microwave Theory Tech ***MTT-13****, 15 (1965).*

[39] *For an analytic treatment, see Elliott*[35] *or D. M. Pozar,* Microwave Engineering, *Sec. 10.6, Addison-Wesley, Reading, MA, 1990.*

[40] *E. F. Schloemann,* Proc. IEEE ***76****, 188 (1988).*

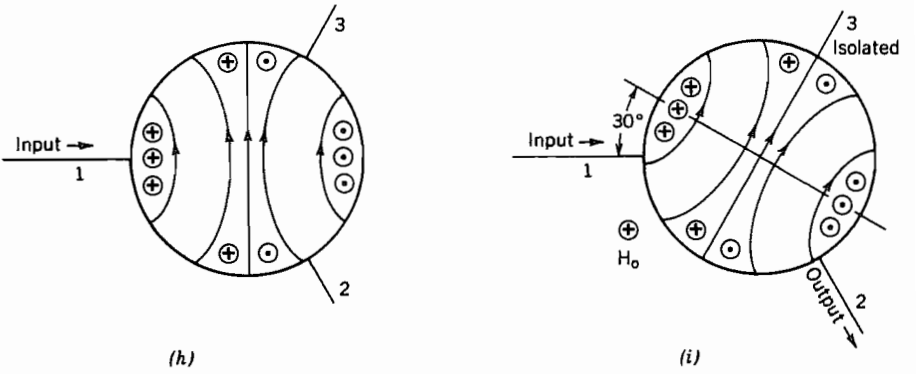

FIG. 13.15 (*h*) Standing-wave pattern in ferrite disk in absence of H_0. (*i*) With selected value of H_0, standing-wave pattern is rotated to isolate line 3. (After Fay and Comstock.[38] © 1965, IEEE.)

13.16 PERMITTIVITY OF A STATIONARY PLASMA IN A MAGNETIC FIELD

In this section we develop explicit, frequency-dependent expressions for the elements of the permittivity matrix of a plasma with an applied steady magnetic field. The results are important in understanding electromagnetic wave propagation through the ionosphere in the presence of the earth's magnetic field, the magnetically confined plasma used in fusion research, and certain laser discharges. Later extensions, with an average electron velocity added, apply to traveling-wave tubes and other electron-beam amplifiers.

Because of the low density of the plasma in comparison with liquids and solids, the primary dielectric behavior is produced by the electron motion. The applied magnetic field causes the permittivity matrix to have off-diagonal elements, since if magnetic field is axial, electron motion in one transverse direction produces forces in the orthogonal transverse direction. The characteristic waves in this case are circularly polarized, as for a ferrite with applied magnetic field seen in the preceding sections.

To bring out the main physical effects, several idealizations are made in the model. The plasma is considered uniform and stationary in this analysis, although later a drift velocity for electrons will be added (Sec. 13.17). Magnetic field is stationary, uniform, and in the z direction. Because of the heavy mass of the ions, their motion is neglected; they serve only to neutralize the dc space-charge fields of the electrons. The effects of thermal velocities and collisions are neglected, as are the forces arising from the magnetic fields of the electromagnetic waves (see Prob. 13.3a).

The first step is to find the convection current in the plasma. The dc plus ac current density is

$$\mathbf{J}_0 + \mathbf{J}_1 = (\rho_0 + \rho_1)(\mathbf{v}_0 + \mathbf{v}_1) \tag{1}$$

Here, $\mathbf{v}_0$ and $\mathbf{J}_0$ are equal to zero since the plasma is assumed stationary. Thus, neglecting products of ac terms since they are of second-order smallness, we see that

$$\mathbf{J}_1 = \rho_0 \mathbf{v}_1 \tag{2}$$

The velocity $\mathbf{v}_1$ is found from the Lorentz equation [Eq. 3.6(5)]

$$\frac{d\mathbf{v}_1}{dt} = -\frac{e}{m}(\mathbf{E} + \mathbf{v}_1 \times \mathbf{B}_0) \tag{3}$$

where $\mathbf{B}_0 = \hat{\mathbf{z}} B_{0z}$ is the applied steady magnetic field.

To find the conditions required for linearization of the equations, let us consider a uniform plane wave having arbitrary direction of propagation, such that the ac spatial variations may be expressed by

$$e^{-j\boldsymbol{\beta}\cdot\mathbf{r}} = e^{-j(\beta_x x + \beta_y y + \beta_z z)} \tag{4}$$

The left side of (3), expanded in partial derivatives and evaluated using (4), becomes

$$\frac{d\mathbf{v}_1}{dt} = j(\omega - \beta_x v_{1x} - \beta_y v_{1y} - \beta_z v_{1z})\mathbf{v}_1 e^{j\omega t} \tag{5}$$

If the ac velocity is assumed to be small compared with any possible phase velocities, then $\beta_i v_{1i} = \omega v_{1i}/v_{pi} \ll \omega$ and (5) reduces to

$$\frac{d\mathbf{v}_1}{dt} \cong j\omega \mathbf{v}_1 e^{j\omega t} \tag{6}$$

Writing (3) in component phasor form using (6), we have

$$j\omega v_{1x} = -\frac{e}{m} E_{1x} - \frac{e}{m} B_{0z} v_{1y} \tag{7a}$$

$$j\omega v_{1y} = -\frac{e}{m} E_{1y} + \frac{e}{m} B_{0z} v_{1x} \tag{7b}$$

$$j\omega v_{1z} = -\frac{e}{m} E_{1z} \tag{7c}$$

Equations (7) may be solved for velocity components in terms of the fields with the result

$$v_{1x} = \frac{-j\omega(e/m)E_{1x} + (e/m)\omega_c E_{1y}}{\omega_c^2 - \omega^2} \tag{8a}$$

$$v_{1y} = \frac{-(e/m)\omega_c E_{1x} - j\omega(e/m)E_{1y}}{\omega_c^2 - \omega^2} \tag{8b}$$

$$v_{1z} = \frac{j(e/m)}{\omega} E_{1z} \tag{8c}$$

where $\omega_c = (e/m)B_{0z}$ is called the angular cyclotron frequency.

It is convenient to define an equivalent flux density **D** that includes the effect of convection currents. In matrix notation, the equivalent displacement current is

$$\begin{aligned} j\omega[D] &= j\omega\varepsilon_0[E] + [J] \\ &= j\omega[\varepsilon][E] \end{aligned} \tag{9}$$

where $[\varepsilon]$ is the equivalent-permittivity matrix. Using (2) and (8),

$$[\varepsilon] = \begin{bmatrix} \varepsilon_{11} & \varepsilon_{12} & 0 \\ \varepsilon_{21} & \varepsilon_{22} & 0 \\ 0 & 0 & \varepsilon_{33} \end{bmatrix} \tag{10}$$

where

$$\varepsilon_{11} = \varepsilon_{22} = \varepsilon_0\left[1 + \frac{\omega_p^2}{\omega_c^2 - \omega^2}\right] \tag{11a}$$

$$\varepsilon_{12} = \varepsilon_{21}^* = \frac{j\omega_p^2(\omega_c/\omega)\varepsilon_0}{\omega_c^2 - \omega^2} \tag{11b}$$

$$\varepsilon_{33} = \varepsilon_0\left[1 - \frac{\omega_p^2}{\omega^2}\right] \tag{11c}$$

Here, ω_p is the plasma frequency, Eq. 13.3(10).

For plane waves in a plasma without a magnetic field (Sec. 13.3), ω_p was observed to be a characteristic frequency in that no propagation occurs for $\omega < \omega_p$. It is clear from the form of (11a) and (11b) that the cyclotron frequency ω_c is also a characteristic frequency in this case. The singularity at ω_c is seen from (8a) and (8b) to result from the singularity in the velocities produced by the wave. A moving electron in a magnetic field without an electric field rotates at an angular frequency ω_c. If an applied alternating electric field oscillates at ω_c, it is so phased on each cycle that it continually pumps the electron to higher and higher velocities. That leads to the infinite response for the continuous-wave case in this model, although collisions would limit excursions in practice.

13.17 Space-Charge Waves on a Moving Plasma with Infinite Magnetic Field

We consider now waves propagating in a plasma parallel to an infinite magnetic field and having a component of electric field in the direction of propagation, as shown in Fig. 13.17. An important application of the results is as a model for waves on electron beams that have an average velocity parallel to the magnetic field. For the purpose of analyzing the space-charge waves, we will first show the effect of v_{0z} on the permittivity matrix developed in Sec. 13.16.

Proceeding as in Eqs. 13.16(9)–(11) yields

$$\varepsilon_{33} = \varepsilon_0\left[1 - \frac{\omega_p^2}{(\omega - \beta v_{0z})^2}\right] \tag{8}$$

Note that the difference in ε_{33} between (8) and that of the stationary plasma, Eq. 13.16(11c), can be considered a Doppler shift in the frequency seen by the electrons. In like manner, the other components of the permittivity matrix can be found by using a Doppler-shifted frequency $\omega - \beta v_{0z}$ wherever ω appears in Eqs. 13.16(11a) and (11b).

Taking the curl of Maxwell's curl **E** equation and substituting the curl **H** equation with a scalar permeability (taking $\mu = \mu_0$) we get [41]

$$\nabla \times \nabla \times \mathbf{E} = \omega^2\mu_0\mathbf{D} \tag{9}$$

Using a common vector identity, this becomes

$$\nabla^2\mathbf{E} - \nabla(\nabla \cdot \mathbf{E}) + \omega^2\mu_0\mathbf{D} = 0 \tag{10}$$

By use of Gauss's law and the assumed $e^{-j\beta z}$ form of variations, the z component of (10) may be written as

$$\nabla_t^2 E_z - \beta^2 E_z + j\beta\frac{\rho_1}{\varepsilon_0} + \omega^2\mu_0\varepsilon_{33}E_z = 0 \tag{11}$$

where $\nabla_t^2 E_z$ contains partial derivatives transverse to the z direction. Combining (3) and (7) we find

$$\rho_1 = -j\frac{\varepsilon_0\omega_p^2\beta}{(\omega - \beta v_{0z})^2}E_z \tag{12}$$

Then combining (11) and (12) and using the value of ε_{33} form (8), we obtain the desired wave equation

$$\nabla_t^2 E_z + (\omega^2\mu_0\varepsilon_0 - \beta^2)\left[1 - \frac{\omega_p^2}{(\omega - \beta v_{0z})^2}\right]E_z = 0 \tag{13}$$

We now restrict our attention to uniform plane longitudinal waves, that is, waves with electric fields along the direction of propagation and no transverse variation. Therefore the first term of (13) vanishes. Equation (13) may then be satisfied if either $\omega^2\mu_0\varepsilon_0 - \beta^2$ or the term in brackets is zero. The first alternative gives the usual TEM *field waves*, with zero E_z. More interesting is the second alternative:

$$1 - \frac{\omega_p^2}{(\omega - \beta v_{0z})^2} = 0 \tag{14}$$

[41] *To get the right side of vector equations like (9) in terms of* **E** *would require tensor or dyadic notation (see footnote 27). We choose to avoid that less familiar notation by using* **D**.

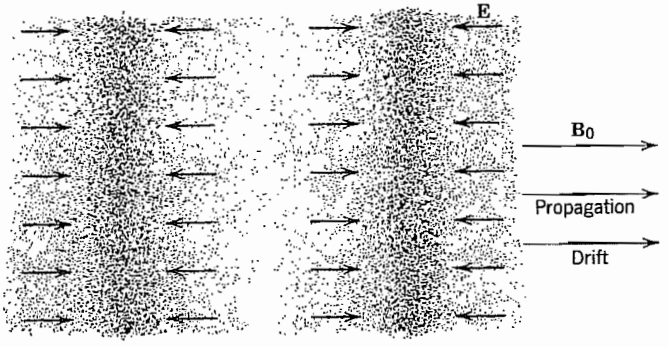

FIG. 13.17 Space-charge waves in a plasma.

The ac current density, Eq. 13.16(1), when linearized, is

$$\mathbf{J}_1 = \rho_0 \mathbf{v}_1 + \mathbf{v}_0 \rho_1 \tag{1}$$

To find ac charge density ρ_1 which arises from the bunching of electrons, we make use of the continuity equation for the ac current density:

$$\nabla \cdot \mathbf{J}_1 = \frac{\partial J_{1x}}{\partial x} + \frac{\partial J_{1y}}{\partial y} + \frac{\partial J_{1z}}{\partial z} = -\frac{\partial \rho_1}{\partial t} \tag{2}$$

With an infinite magnetic field, $J_{1x} = J_{1y} = 0$. Then with all ac quantities having wave form, $e^{j(\omega t - \beta z)}$, (2) gives

$$\rho_1 = \frac{\beta J_{1z}}{\omega} \tag{3}$$

To get the value of v_{1z} needed in (1), we return to the force equation Eq. 13.16(3) and write the z component of the left side, taking account of the average velocity v_{0z}:

$$\frac{dv_{1z}}{dt} = \frac{\partial v_{1z}}{\partial t} + v_{0z} \frac{\partial v_{1z}}{\partial z} \tag{4}$$

Noting that $\mathbf{v}_1 \times \mathbf{B} = 0$, the force equation becomes, in phasor form,

$$j(\omega - \beta v_{0z}) v_{1z} = -\frac{e}{m} E_{1z} \tag{5}$$

or

$$v_{1z} = \frac{j(e/m)}{\omega - \beta v_{0z}} E_{1z} \tag{6}$$

Substituting (3) and (6) into (1) and using the definition of the plasma frequency ω_p in Eq. 13.3(10), we get

$$J_{1z} = \frac{-j\omega\varepsilon_0\omega_p^2}{(\omega - \beta v_{0z})^2} E_{1z} \tag{7}$$

This leads to two waves with phase constants

$$\beta_{1,2} = \frac{\omega \pm \omega_p}{v_{0z}} \tag{15}$$

These waves involve interaction with the electrons and are called *space-charge waves.*[42] Typically, $\omega_p \ll \omega$, and we may use the binomial expansion to obtain the phase velocities in the form

$$(v_p)_{1,2} = \frac{\omega}{\beta_{1,2}} \approx v_{0z}\left(1 \mp \frac{\omega_p}{\omega}\right) \tag{16}$$

the values of which are seen to be somewhat greater and somewhat less than the drift velocity v_{0z}. The group velocity is

$$v_g = \frac{\partial \omega}{\partial \beta} = v_{0z} \tag{17}$$

for both space-charge waves. With the plasma drift v_{0z} reduced to zero, a perturbation of the electron charge density leads to a local oscillation at a frequency $\omega = \omega_p$, but the effect does not propagate.

13.18 TEM Waves on a Stationary Plasma in a Finite Magnetic Field

Many types of waves can propagate in a plasma with an applied magnetic field, including hybrid TE and TM modes.

Here we restrict our attention to simple TEM waves propagating parallel to the applied dc magnetic field. The magnetized plasma is a gyrotropic medium so the normal modes of propagation are circularly polarized waves.

The TEM wave has no E_z component and no variations of fields with respect to transverse coordinates, so $\nabla \cdot \mathbf{E} = 0$ and Eq. 13.17(10) may be written in matrix form:

$$\frac{d^2}{dz^2}\begin{bmatrix} E_x \\ E_y \\ 0 \end{bmatrix} + \omega^2\mu_0\begin{bmatrix} \varepsilon_{11} & \varepsilon_{12} & 0 \\ \varepsilon_{21} & \varepsilon_{22} & 0 \\ 0 & 0 & \varepsilon_{33} \end{bmatrix}\begin{bmatrix} E_x \\ E_y \\ 0 \end{bmatrix} = \begin{bmatrix} 0 \\ 0 \\ 0 \end{bmatrix} \tag{1}$$

In the analysis of ferrites in Sec. 13.13, we saw that circularly polarized waves having the same direction of rotation with respect to the dc magnetic field have the same characteristic wave impedance and the same propagation constant; that result also applies here.

[42] *S. Ramo,* Phys. Rev. ***56****, 276 (1939); the concept was first usefully applied to electron devices by W. C. Hahn,* Gen. Elect. Rev. ***42****, 258, 497 (1939).*

Consider first the waves having clockwise rotation relative to the dc magnetic field:

$$\mathbf{E}_+^{cw} = E_+^{cw}(\hat{\mathbf{x}} - j\hat{\mathbf{y}}), \qquad \mathbf{E}_-^{ccw} = E_-^{ccw}(\hat{\mathbf{x}} - j\hat{\mathbf{y}}) \tag{2}$$

If the electric fields in (2) are substituted into Maxwell's curl **E** equation, we obtain the corresponding magnetic fields

$$\mathbf{H}_+^{cw} = H_+^{cw}(j\hat{\mathbf{x}} + \hat{\mathbf{y}}), \qquad \mathbf{H}_-^{ccw} = -H_-^{ccw}(j\hat{\mathbf{x}} + \hat{\mathbf{y}}) \tag{3}$$

If either of Eqs. (2) is substituted into (1), we find the propagation constant

$$\beta_1 = \omega\sqrt{\mu_0}\,(\varepsilon_{11} - j\varepsilon_{12})^{1/2} = \omega\sqrt{\mu_0\varepsilon_0}\left(1 + \frac{\omega_p^2/\omega}{\omega_c - \omega}\right)^{1/2} \tag{4}$$

and the characteristic wave impedance is given by

$$\eta_1 = \frac{E_+^{cw}}{H_+^{cw}} = \frac{E_-^{ccw}}{H_-^{ccw}} = \sqrt{\frac{\mu_0}{\varepsilon_{11} - j\varepsilon_{12}}} = \sqrt{\frac{\mu_0}{\varepsilon_0\left(1 + \dfrac{\omega_p^2/\omega}{\omega_c - \omega}\right)}} \tag{5}$$

These relations can be used in the transmission-line analogy as was done for ferrites in Sec. 13.13 by writing expressions analogous to the voltage and current in transmission lines and introducing the impedance concept. The total electric and magnetic fields are

$$E_1(z) = E_+^{cw}e^{-j\beta_1 z} + E_-^{ccw}e^{j\beta_1 z} \tag{6}$$

$$H_1(z) = \frac{1}{\eta_1}(E_+^{cw}e^{-j\beta_1 z} - E_-^{ccw}e^{j\beta_1 z}) \tag{7}$$

wherein β_1 is given by (4) and η_1 by (5). To complete the analogy we need to define the total impedance

$$Z_1(z) = \frac{E_1(z)}{H_1(z)} \tag{8}$$

Then all the methods of transmission-line analysis can be applied to problems involving discontinuities of medium perpendicular to the direction of propagation.

There is also a pair of wave solutions in which the fields rotate counterclockwise with respect to the direction of the dc magnetic field. The quantities corresponding to equations (2)–(8) are

$$\mathbf{E}_+^{ccw} = E_+^{ccw}(\hat{\mathbf{x}} + j\hat{\mathbf{y}}), \qquad \mathbf{E}_-^{cw} = E_-^{cw}(\hat{\mathbf{x}} + j\hat{\mathbf{y}}) \tag{9}$$

$$\mathbf{H}_+^{ccw} = H_+^{ccw}(-j\hat{\mathbf{x}} + \hat{\mathbf{y}}), \qquad \mathbf{H}_-^{cw} = H_-^{cw}(j\hat{\mathbf{x}} - \hat{\mathbf{y}}) \tag{10}$$

$$\beta_2 = \omega\sqrt{\mu_0}(\varepsilon_{11} + j\varepsilon_{12}) = \omega\sqrt{\mu_0\varepsilon_0}\left(1 - \frac{\omega_p^2/\omega}{\omega_c + \omega}\right)^{1/2} \tag{11}$$

$$\eta_2 = \frac{E_+^{\text{ccw}}}{H_+^{\text{ccw}}} = \frac{E_-^{\text{cw}}}{H_-^{\text{cw}}} = \sqrt{\frac{\mu_0}{\varepsilon_{11} - j\varepsilon_{12}}} = \sqrt{\frac{\mu_0}{\varepsilon_0\left(1 - \dfrac{\omega_p^2/\omega}{\omega_c + \omega}\right)}} \tag{12}$$

$$E_2(z) = E_+^{\text{ccw}} e^{-j\beta_2 z} + E_-^{\text{cw}} e^{j\beta_2 z} \tag{13}$$

$$H_2(z) = \frac{1}{\eta_2}\left(E_+^{\text{ccw}} e^{-j\beta_2 z} - E_-^{\text{cw}} e^{j\beta_2 z}\right) \tag{14}$$

$$Z_2(z) = \frac{E_2(z)}{H_2(z)} \tag{15}$$

If a linearly polarized wave is incident on a gyrotropic medium, it can be decomposed into two counterrotating circularly polarized waves and each can be analyzed by the transmission-line methods. This applies for the plasma as well as for ferrite media. The procedures were discussed at the end of Sec. 13.13.

PROBLEMS

13.2a The susceptibility χ_e of nitrogen at 20°C and atmospheric pressure is about 5.5×10^{-4}. What molecular polarizability α_T does this correspond to? Assuming the ideal gas law, and α_T independent of temperature, give susceptibility as a function of temperature.

13.2b Find the resonant frequency for an electronic resonance (charge cloud in an atom) in the Lorentz model, assuming the atom to have 10 electrons distributed uniformly in the cloud and acting as a group. The maximum displacement r of the charge cloud from the equilibrium position is less than its radius $a = 0.1$ nm.

13.2c Consider a liquid with $\varepsilon_r = 4.0$ at room temperature for dc fields. Take the polarization **P** to be proportional to **E**. Assume, for simplicity, that the polarizability results only from orientation of permanent dipoles and that there is spherical symmetry about each molecule. The density of molecules is 10^{28} m^{-3} and the relaxation time 10^{-11} s. Find the dc polarizability and the field frequency at which $\varepsilon' = 2.0\varepsilon_0$.

13.2d* Find from Eq. 13.2(11) the corresponding permittivity with g and Γ taken as real and frequency independent. Show that ε' and ε'' satisfy the Kramers–Kronig relations, Eqs. 13.2(13) and (14). Assume small damping; use limits $-\infty$ to ∞ as in Eq. 11.11(5).

13.2e* Repeat Prob. 13.2d for a permittivity based solely on Eq. 13.2(12).

13.3a Show that the ratio of magnetic to electric forces on the electrons in an ionized gas resulting from the fields of a uniform plane wave is v/v_p, where v is electron velocity and v_p is the phase velocity of the wave. Assume a 10-MHz wave carrying a power of 1 W/m^2 and estimate the maximum electron velocity, assuming negligible collision frequency. Give an upper limit for v/v_p in this case. Assume $\omega \gg \omega_p$.

13.3b Assume a neutral plasma in which all electrons in the region x to $x + \Delta x$ are given a displacement Δx. Considering the forces acting to restore neutrality, show that the displaced sheet will oscillate at the "plasma frequency" ω_p given by Eq. 13.3(10).

13.3c A sample of silicon ($\varepsilon_1 = 11.7\varepsilon_0$) uniformly doped n-type with a dopant concentration of 5×10^{17} cm^{-3} is found to have a dc conductivity of 2.5×10^3 S at $T = 300$ K. The electron effective mass is $0.26m_0$ where m_0 is the electron rest mass. Determine the collision frequency, assuming that the electron density equals the dopant density. Find the frequency at which ε'' differs from the value in Eq. 13.3(8) by 10%. Evaluate the ratio of second to first terms on the right side of Eq. 13.3(6) where $\omega \to 0$ and $\omega = \nu$. Comment on the restrictions on the use of Eq. 13.3(8).

13.3d A simple model of the ionosphere may be formulated by assuming that the number density of free electrons increases linearly from zero at height z_0 to 10^{12} per cubic meter at height z_1 and then decreases linearly to zero at height $2z_1 - z_0$. The collisions may be neglected. A uniform plane wave traveling directly upward encounters the ionosphere. What is the highest frequency for which this wave will be totally reflected? Plot the maximum altitude versus frequency.

13.3e Find the real and imaginary components of the dielectric constant, ε' and ε'', respectively, of silver and nickel for waves from a CO_2 laser (10.6-μm wavelength) using Fig. 13.3*b*, assuming the complex behavior can be cast in that form. Determine the ratio of the magnitudes of the real and imaginary components of total current.

13.3f Plot attenuation in nepers/micrometer versus wavelength for nickel and silver over the wavelength range of Fig. 13.3*b*, using data of that figure.

13.3g Plot curves of n_r and n_i versus wavelength for silver assuming it a good conductor with the conductivity given in Table 3.17, and compare with Fig. 13.3*b* over the wavelength range shown. Comment on reasons for differences.

13.4a As discussed in Sec. 13.4, time-dependent fields decay into the surface of a collisionless conductor if $\omega < \omega_p$. Show this from Maxwell's equations in time-dependent form using Eq. 13.3(1) with $\nu = 0$ and $dv/dt \approx \partial v/\partial t$. Specifically, show that

$$\left(\frac{\partial B_x}{\partial t}\right)_z = \left(\frac{\partial B_x}{\partial t}\right)_{z=0} \exp(-\alpha z)$$

where $\alpha^2 = \mu n_e e^2/m$ and B_x is tangential to the plane surface of a half-space as in Fig. 13.4.

13.4b* The *two-fluid model* of a superconductor assumes that a portion n_n of the total electron concentration is in the normal state described by Eq. 13.3(1) and the remainder n_s is in the superconducting state for which $m\, d\mathbf{v}_s/dt = -e\mathbf{E}$. Calculate current density for each component and add to get $\mathbf{J}_{total} = \sigma\mathbf{E}$. Show that for $(\omega/\nu)^2 \ll 1$, $n_n \lesssim n_s$ and $n = n_s + n_n$, $\sigma = \sigma_n(n_n/n) - j(1/\omega\mu\lambda_L^2)$ where $\sigma_n = ne^2/\nu m$. Use the usual expression for skin depth to show that

$$\delta = \sqrt{2}\lambda_L \left[\left(\frac{\omega}{\nu}\right)\left(\frac{n_n}{n_s}\right) - j\right]^{-1/2}$$

and that in the low-frequency limit $\exp[-(1 + j)z/\delta]$ becomes $\exp(-z/\lambda_L)$.

13.4c Bulk superconductors (dimensions very large compared with penetration depth) are often considered to be perfectly diamagnetic ($\mu = 0$). Use the analysis in Sec. 7.18 to show that a sphere of superconducting material in an otherwise uniform magnetic field will have $B = 0$ inside and $H = \frac{3}{2}H_0$ at the equator at $r = a$.

13.4d Using the energy method, calculate the inductance per unit length of a parallel-plate superconducting transmission line. Assume the plates are identical, are much thicker than the penetration depth λ_L, and are wide enough to neglect fringing. You should find $L = (\mu_0/w)(\lambda_L + d)$, where w is the width and d the dielectric thickness. [*Note:* The kinetic energy of the collisionless superconducting electron fluid contributes to the inductance an amount equal to the magnetic energy inside the superconductors. Thus, the correct inductance is $L = (\mu_0/w)(2\lambda_L + d)$.]

13.4e Suppose a quasi-TEM wave propagates in a parallel-plate structure in which thick superconducting electrodes are spaced by (3 nm) niobium oxide having a relative permittivity of 30.

(i) Use the correct expression for L given in Prob. 13.4d to find an expression for the phase velocity of this transmission line.

(ii) Find v_p for the given structure assuming $\lambda_L = 0.039$ μm for niobium and compare with the velocity of a plane wave in the same dielectric.

(iii) How would the result differ if niobium were a collisionless conductor?

13.5a* The potential energy of a dipole in a magnetic field H_i is $-m_0\mu_0 H_i \cos\theta$, where θ is the angle between m_0 and H_i. Boltzmann theory states that the relative probability of finding a dipole with an energy U is given by $\exp(-U/kT)$. Write an expression for the average value of the component of dipole moment in the direction of H_i, $\langle m_0 \cos\theta\rangle$, and do the integrations to show the validity of Eq. 13.5(3).

13.5b Magnetic dipole moment of a small current loop of radius a is $m_0 = \pi a^2 I$ (Sec. 2.10). Verify that the argument of the hyperbolic contangent in Eq. 13.5(3) and χ_m are dimensionless.

13.6a Spontaneous magnetization can only occur if there is some value of H_i for which Eqs. 13.5(3) and 13.6(1) are simultaneously satisfied. Sketch roughly the forms of these two expressions as functions of H_i, indicating a point of intersection. As temperature is raised, the point of intersection moves to lower H_i. The highest temperature at which there is a simultaneous solution is the Curie temperature T_c. At this temperature the initial slopes of the two curves are equal. Use this fact to find a relation between κ and T_c.

13.6b Find κ for iron using the result of Prob. 13.6a and Curie temperature of 1043 K. There are 8.6×10^{22} atoms/cm^3. Assume that the magnetic moment of the iron atom is 2.22 Bohr magnetons, where a Bohr magneton is $eh/4\pi m$. Here e is the electronic charge, h is Planck's constant (6.63×10^{-34} J-s), and m is the mass of an electron.

13.6c For the material depicted by Fig. 13.6*d* assume $B_{sat} = 0.1$ T. Deduce the scale on the H axis and estimate the energy loss per cycle if H is swept through the range shown. Find values for coercive force, remanence, initial permeability, and maximum permeability. (Note that since Fig. 13.6*d* is only diagrammatric, numbers obtained will not be representative of real materials.)

13.6d Assume that a rod of circular cross section of radius a and length l has been uniformly magnetized parallel to its axis. Find the current per meter in a solenoid of the same length to get the same flux density at the ends on the axis. Write an expression for the magnetic flux density on the axis at the end of the rod.

13.6e When an ellipsoidal sample of isotropic magnetic material is placed in an otherwise uniform magnetic field H_{app}, a complex field distribution results outside the sample but it is uniform inside. If the field is along a principal axis of the ellipsoid the field

inside is parallel with H_{app} and its magnitude is given by a *demagnetization factor* $\mathfrak{D}$ and the *constitutive relation* between B and H:

$$H = \frac{H_{app} - \mathfrak{D}B/\mu_0}{(1 - \mathfrak{D})}$$

(i) A rod of circular cross section is modeled by a long prolate ellipsoid of revolution with **H** perpendicular to the long axis, $\mathfrak{D} = \frac{1}{2}$. Suppose a rod of $\mu = 100$ material in this arrangement and find the ratio of internal B to applied $B = \mu_0 H_{app}$.

(ii) Show that the result for a sphere in Eq. 7.18(25) can be found from the above relation with $\mathfrak{D} = \frac{1}{3}$.

(iii) Verify the result for a superconducting sphere given in Prob. 13.4c.

(iv) Argue from boundary conditions why $\mathfrak{D} = 0$ for field parallel with major axis of a long prolate ellipsoid of revolution.

13.7 Suppose two coparallel waves with the same electric field polarization pass through a 1-cm-long crystal. The fields are intense and produce nonlinear effects. The wavelengths (in free space) of the waves are 632.8 and 592.1 nm.

(i) What is the maximum difference in index n between $\omega_1 - \omega_2$ and ω_1 [assume $n(\omega_1) = n(\omega_2)$] if negligible cancellation is to occur because of the difference of phase constants between the polarization and the wave propagating at $\omega_1 - \omega_2$. Use as a criterion that the difference integrated over the length of the crystal is not greater than $\pi/2$.

(ii) An output difference-frequency wave of 1.0 mW is observed. What is the power lost or gained by each of the two driving waves?

13.8a As a simple example of the idea of diagonalizing matrices by coordinate transformations, consider a two-dimensional system where

$$\begin{bmatrix} D_x \\ D_y \end{bmatrix} = \varepsilon_0 \begin{bmatrix} 1.75 & 0.433 \\ 0.433 & 1.25 \end{bmatrix} \begin{bmatrix} E_x \\ E_y \end{bmatrix}$$

Write expressions for **D** and **E** in a primed coordinate system rotated by θ from the unprimed system. By combining these with the given relation between **D** and **E**, find the amount of rotation necessary to put $[\varepsilon]$ in the diagonal form

$$[\varepsilon] = \varepsilon_0 \begin{bmatrix} 1 & 0 \\ 0 & 2 \end{bmatrix}$$

13.8b Barium titanate ($BaTiO_3$) has $\varepsilon_{11} = \varepsilon_{22} = 5.94\varepsilon_0$ and $\varepsilon_{33} = 5.59\varepsilon_0$. Sketch (showing dimensions) and describe the index ellipsoid. What are the values of X, Y, and Z that pertain to a plane wave propagating in the y direction with its **D** vector in the z direction?

13.8c Show that Eq. 3.12(6) is consistent with Eq. 3.15(5) for linear, anisotropic, time-invariant media, as was done in Prob. 3.12f for isotropic media.

13.9a Derive Eq. 13.9(4).

13.9b Verify the conversion of Eq. 13.9(10) to Eq. 13.9(12), the "Fresnel equation of wave normals."

13.9c* Assume waves propagating with direction such that $b_x = 0.900$, $b_y = 0.100$, and $b_z = 0.424$ in a crystal with $\mu = \mu_0$ and $\varepsilon_{11} = 12\varepsilon_0$, $\varepsilon_{22} = 14\varepsilon_0$, and $\varepsilon_{33} = 16\varepsilon_0$.

Determine the values of phase velocity for the two allowed waves. Find for each the vector expressions for $\mathbf{D}$ and show that $\mathbf{D}_1 \perp \mathbf{D}_2$.

13.9d* For the index ellipsoid shown in Fig. 13.9*c* with an arbitrary propagation direction $\boldsymbol{\beta}$, show that if an ellipse is defined by the intersection of the ellipsoid and a plane normal to $\boldsymbol{\beta}$, major and minor axes of the ellipse define two basic solutions for the direction of $\mathbf{D}$, and corresponding indices of refraction. [*Hint:* Find the extrema of $R^2 = X^2 + Y^2 + Z^2$ subject to the two constraints on X, Y, Z, on the boundary of the intersection ellipse using Lagrange multipliers. This will lead to three equations of the form $X(1 - R^2/n_x^2) + b_x R^2[(Xb_x/n_x^2) + (Yb_y/n_y^2) + (Zb_z/n_z^2)]$, where $n_x^2 = \varepsilon_{11}/\varepsilon_0$, etc., which can be recast into the form of Eqs. 13.9(8).]

13.10a A beam of light is normally incident on a surface of a calcite ($CaCO_3$) crystal as shown in Fig. 13.10*b*. The optical axis is at an angle 29 degrees from the inward surface normal. Take $\varepsilon_{11} = \varepsilon_{22} = 2.7\varepsilon_0$ and $\varepsilon_{33} = 2.2\varepsilon_0$. Treat the incident light as unpolarized plane waves. Find the spatial separation of ordinary and extraordinary rays at the opposite (parallel) crystal surface 1 cm away.

13.10b For a beam of light incident at an oblique angle on a planar slab of double-refracting (birefringent) material, show that the two emergent rays are parallel.

13.10c* A linearly polarized wave at $\lambda_0 = 550$ nm is incident with its electric field at 45 degrees to the y axis on the surface of a 1.0-μm slab of $LiNbO_3$ cut so that y–z plane lies in the surface ("x-cut"). Indices are $n_o = 2.29$ and $n_e = 2.20$. Find the wave propagated beyond the slab.

13.11a Show that the new principal axes x' and y' are rotated by 45 degrees from the crystal axes x and y when a crystal of KDP is subjected to an electric field E_z. Prove that the 11 and 22 elements of the $[1/n^2]$ matrix in the primed coordinate system are given by Eqs. 13.11(10).

13.11b A $BaTiO_3$ crystal is to be used as a modulator as shown for $LiNbO_3$ in Ex. 13.11a. Assume the light is polarized with $\mathbf{E} = \hat{\mathbf{x}}E_x$ and find the magnitude of field required for π rad of phase shift. Note the large value of r_{42} for $BaTiO_3$. Take $\lambda = 550$ nm and $l = 1$ cm. How would you orient wave propagation direction, polarization, and direction of modulating field with respect to crystal axes to make use of this coefficient?

13.11c As noted in the discussion of the modulator of Fig. 13.11*c*, a "quarter-wave" plate may be used to bring the ratio of $|E_z(l)/E_x(0)|$ to the linear portion of the variation (Fig. 13.11*d*). Calculate for $\lambda = 550$ nm the basic thickness for KDP with $n_e = 1.47$ and $n_o = 1.51$ and for quartz with $n_e = 1.55$, $n_o = 1.54$. (Since these are small values, full wavelengths are added or the thin sheets placed between thicker, transparent isotropic materials).

13.12a Assume a model of an electron as a spinning sphere of uniform mass and charge and calculate its magnetic moment and angular momentum. Show that γ in Eq. 13.12(2) differs by a factor of 2 from the value given in the text.

13.12b Verify the matrix coefficients in Eq. 13.12(13) and (14) starting with 13.12(9).

13.13a** Consider a 10-cm-thick plane slab of ferrite of infinite cross section normal to the z axis. Assume a dc z-directed magnetic field H_0 of 10^5 A/m inside the ferrite. The saturation magnetization M_0 of the ferrite is 1.5×10^5 A/m and the relative permittivity is 13. A linearly polarized plane wave of frequency 10^9 Hz moving in the $+z$ direction is incident on the slab. Find the wave on the other side of the slab in terms of the incident wave using transmission-line methods.

13.13b The literature on ferrite properties often gives saturation magnetization as $4\pi M_0$ and magnetic field H_0 in gaussian units. Calculate the gaussian values of $4\pi M_0$ and H_0 from the MKS values of M_0 and H_0 given in Prob. 13.13a. Also equate values of ω_0 for the two systems of units to show that γ in the expression $\omega_0 = -\gamma H_0$ using gaussian units has the value -1.76×10^7 rad/O-s.

13.14a Show that Faraday rotation for a wave traveling in the $-z$ direction is in the same direction relative to the magnetic field as for a wave in $+z$ direction. Sketch the orientation of **H** for various z at $t = 0$ in the wave in $-z$ direction.

13.14b Show that Eq. 13.11(13) represents an elliptically polarized wave and contrast with the Faraday effect.

13.14c Some materials possess a property called *natural optical rotation* whereby the plane of polarization of a wave passing through them is rotated without the application of electric or magnetic fields. This is explained by the "screw-like" nature of individual molecules. For example, a 10-cm column of a cane sugar solution (0.1 g/cm^3) produces about 6.7 degrees of rotation. Assuming the individual molecules to be represented crudely by right-hand screws, explain why there remains a net effect in a solution where these molecules are randomly oriented. Explain also why the reflected wave returns to its original polarization, in contradistinction to the Faraday effect where the reflected wave rotates through an additional angle. What should be the rotation per meter of a 0.05 g/cm^3 solution of sugar?

13.15 Consider a resonance isolator in a rectangular waveguide. Operating frequency is 18 GHz in TE_{10} mode at 1.3 times its cutoff frequency. Absorbing strip is square cross section; approximate as a circular rod and use information in Prob. 13.6e. Assume B saturated at 0.2 T. Determine location of strip and magnitude and sign of the applied field H_{app}.

13.16a Assume plane waves propagating in the z direction in a plasma so that $E_z = 0$, in the case where there is an average drift velocity v_0 of the electrons in the z direction parallel to the steady magnetic field. Find ε_{11}, ε_{12}, ε_{21} and ε_{22}. Note in the result that the electrons see a field with Doppler shifted frequency.

13.16b Repeat the derivation of Sec. 13.16 to find the permittivity matrix taking account of the motion of singly charged ions of mass m_i as well as the electrons.

13.17a Evaluate the propagation constants in Eq. 13.17(15) for a beam of electrons which has been accelerated to an energy of 2000 eV. The current density is 10^5 A/m^2. Plot an $\omega - \beta$ diagram for the space-charge waves. For convenience use $\omega\sqrt{\mu_0\varepsilon_0}$ as the ordinate.

13.17b Consider a plasma with electrons drifting along an infinite magnetic field as in Sec. 13.17 but located inside a circular cylindrical waveguide with perfect-conductor walls. Use the differential equation 13.17(13) in the appropriate form to find an expression for the cutoff frequencies of the allowed electromagnetic modes.

13.18a A linearly polarized plane wave with equal y and z components of electric field is launched in the x direction in a neutral plasma with infinite magnetic field in the z direction. The frequency is 4 GHz and the number density of electrons is 10^{17} per cubic meter. Find the distance in which the linearly polarized wave becomes circularly polarized.

13.18b* A beam of millimeter waves (100 GHz) is normally incident on a 0.06-mm-thick planar metal membrane in air. The temperature of the membrane is low enough to neglect collisions of the electrons. An extremely strong (assume infinite) steady

magnetic field $\mathbf{B}_0$ is applied to the membrane with $\mathbf{B}_0$ parallel to the surface. Take electron density to be 10^{23} cm^{-3}, permittivity of the ions as $30\varepsilon_0$, and $\mathbf{E}$ in the incident wave to be 45 degrees from $\mathbf{B}_0$. Find the magnitude of the wave that exists beyond the membrane.

13.18c Suppose a stationary plasma filling the half-space $z > 0$ in a magnetic field in the $+z$ direction. The other half-space $z < 0$ has only vacuum. Take the number density of electrons to be 10^{17} m^{-3} and the magnetic field to be 0.1 T. A clockwise polarized plane wave of frequency 2 GHz propagating in the $+z$ direction is incident on the plasma. What is the value of the field of the wave propagating in the plasma as a fraction of the field in the incident wave?

13.18d Sketch the variations of β_+^{cw} and β_+^{ccw} versus ω in the frequency ranges where propagation occurs. Identify the values of ω at the edges of the propagation ranges.

13.18e For a plasma with electron density of 10^{16} m^{-3}, plot the angle of Faraday rotation in radians per meter of a linearly polarized wave at 3 GHz propagating parallel to constant $\mathbf{B}$ for $B = 0$ to $B = 0.09$ T. What happens when $B = 0.1$ T?

13.18f* A linearly polarized plane wave in free space is incident normal to a planar layer of plasma 10 cm thick. The region beyond the plasma layer is also free space. Assume electron density, magnetic field, and frequency as in Prob. 13.18c. Find the electric field of the wave reflected from the plasma.